Accelerators of charge particles – the power instrument for investigation of radiation resistance and development of new materials of nuclear power

O.V. Borodin, V.V. Bryk, V.F.Zelensky, I.M. Neklyudov, V.N. Voyevodin

Department of Radiation Damage and Material Science
National Science Center
"Kharkov Institute of Physics and Technology"

(voyev@kipt.kharkov.ua)

Nuclear renaissance - materials problems

- The problem of material development for operation in unique conditions of irradiation and evaluation of their radiation resistance consists in the use of existing irradiation facilities for determination of mechanisms of radiation damage and selection of materials with high radiation resistance.
- Unfortunately structural materials in the nuclear power plants undergo degradation due to irradiation influence. Rate of degradation of nuclear materials tends to accelerate due to irradiation.
- While neutron irradiations are essential to evaluate and qualify materials for Generation IV systems, it is important to note that effective radiation effects experiments can be performed using ion-beam facilities.. These facilities are very useful for studying microstructural and microchemical changes during irradiation as well as corrosion and mechanical properties in many circumstances.
- Charged particles irradiations can provide a low-cost method for conducting valuable radiation effects research in absence of, or as a precursor to verification experiments in reactors.

Advantage of ion and electron simulation

Why accelerators are needed?

- Higher damage rate
- Good control of experimental parameters (temperature, flux and environment), possibility of parameters separation
- Ideally suited for optimizing minor alloying composition
- Only one possible choice in the absence of high flux neutron irradiation facility. Many nuclear facilities are shut down now (FFTF, RAPSODIE, DFR, PFR, Superfenix, EBR-II etc)
- Irradiated specimens are not radioactive, unlike reactor specimens which are highly radioactive and may have to be handled only in hot cells

Radiation damage by 1 MeV particles

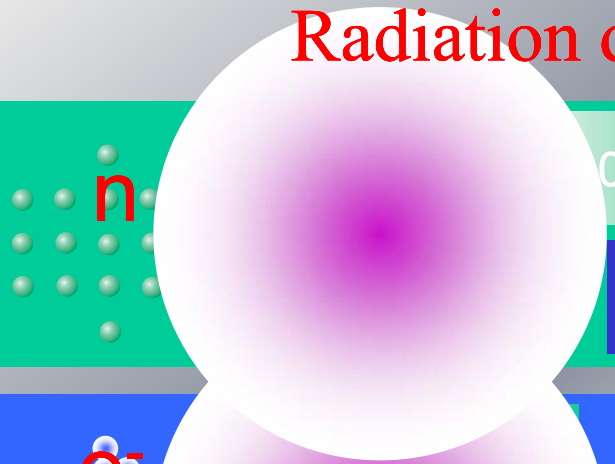

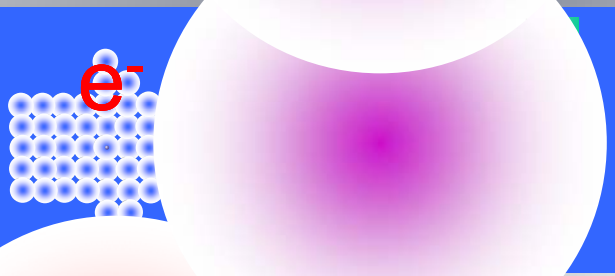

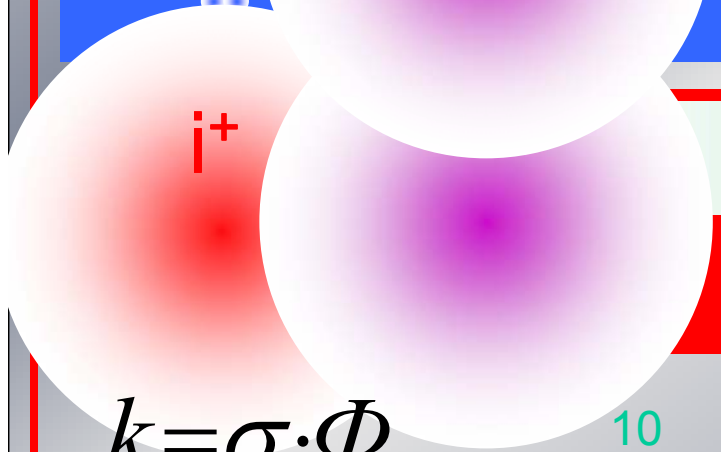

$$k = \sigma \cdot \Phi$$

$$\left[\frac{dpa}{s}\right] = [cm^2] \cdot \left[\frac{particle}{cm^2 \cdot s}\right]$$

$$1barn = 10^{-24} cm^2$$

Advantage of ion and electron simulation

Why accelerators are needed?

- Higher damage rate
- Good control of experimental parameters (temperature, flux and environment), possibility of parameters separation
- Ideally suited for optimizing minor alloying composition
- Only one possible choice in the absence of high flux neutron irradiation facility. Many nuclear facilities are shut down now (FFTF, RAPSODIE, DFR, PFR, Superfenix, EBR-II etc)
- Irradiated specimens are not radioactive, unlike reactor specimens which are highly radioactive and may have to be handled only in hot cells

Fluence and dose distribution along active zone of BOR-60 reactor

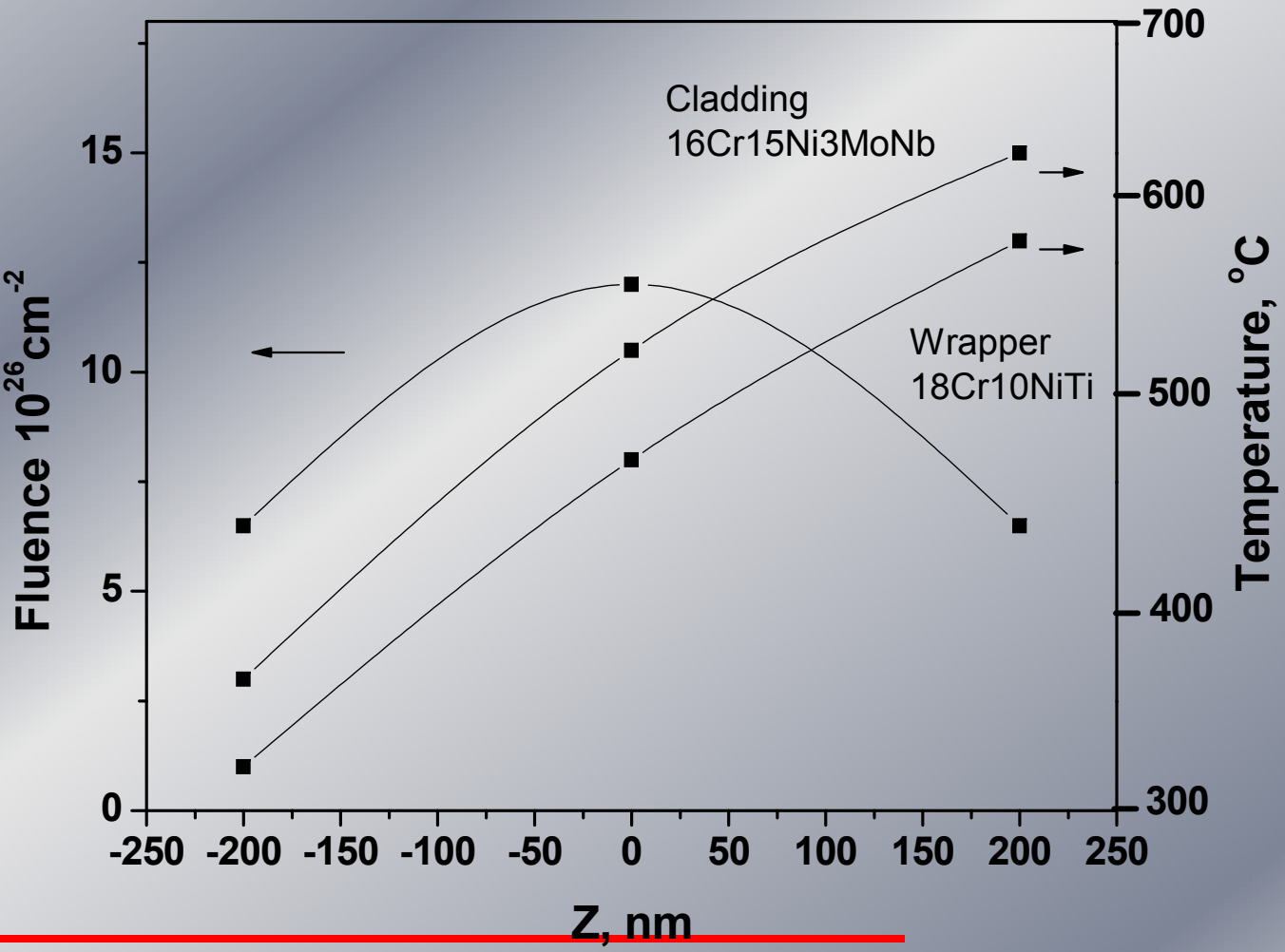

Advantage of ion and electron simulation

Why accelerators are needed?

- Higher damage rate
- Good control of experimental parameters (temperature, flux and environment), possibility of parameters separation
- Ideally suited for optimizing minor alloying composition
- Only one possible choice in the absence of high flux neutron irradiation facility. Many nuclear facilities are shut down now (FFTF, RAPSODIE, DFR, PFR, Superfenix, EBR-II etc)
- Irradiated specimens are not radioactive, unlike reactor specimens which are highly radioactive and may have to be handled only in hot cells

Swelling versus concentration of REE elements in Ni. T_{irr}=600ºC, D=40dpa, E=2.8MeV.

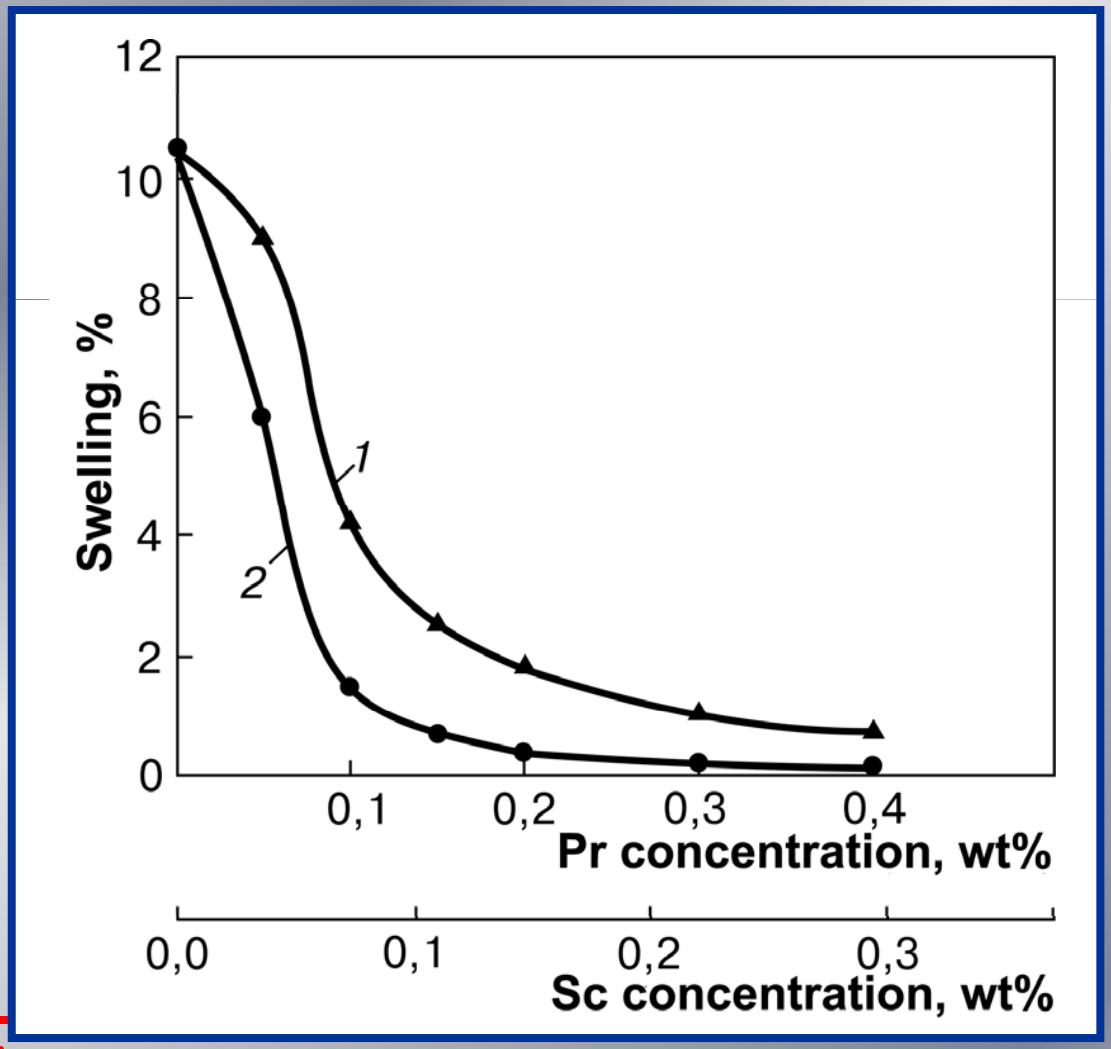

Why accelerators are needed?

Advantage of ion and electron simulation

- Higher damage rate
- Good control of experimental parameters (temperature, flux and environment), possibility of parameters separation
- Ideally suited for optimizing minor alloying composition
- Only one possible choice in the absence of high flux neutron irradiation facility. Many nuclear facilities are shut down now (FFTF, RAPSODIE, DFR, PFR, Superfenix, EBR-II ,BR-10,BN-350etc).Now toohigh duration and cost needed for irradiation of materials up to very high burnups
- Irradiated specimens are not radioactive, unlike reactor specimens which are highly radioactive and may have to be handled only in hot cells

ION SIMULATION OF NEUTRON DAMAGE

Damage Efficiency

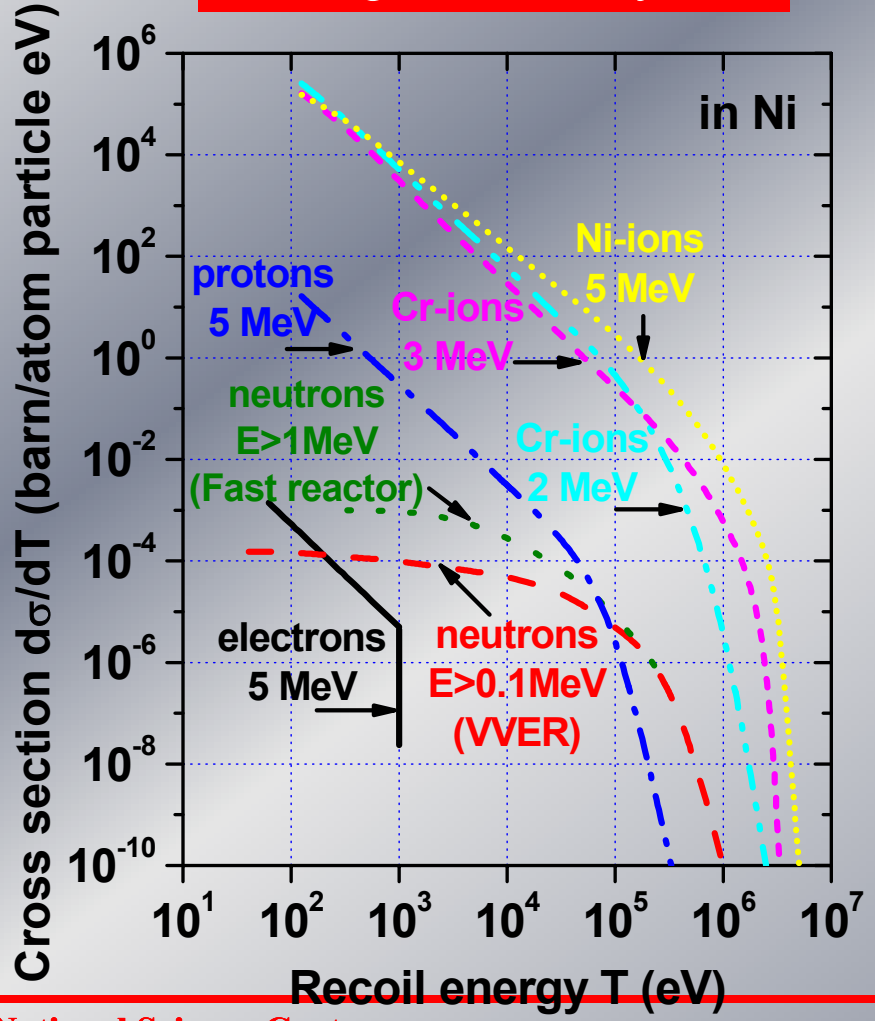

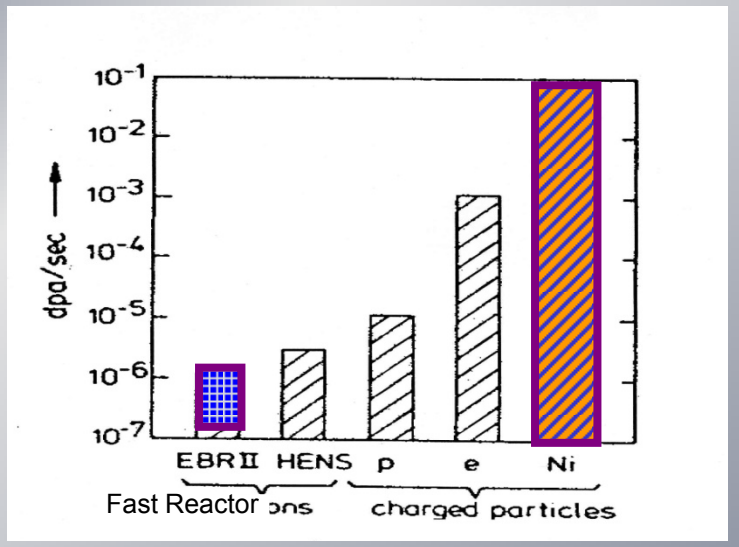

ION BEAMS CAN PRODUCE DISPLACEMENT DAMAGE AT A MUCH FASTER RATE THAN NEUTRONS

KIPT ion and electron accelerators (2000 year)

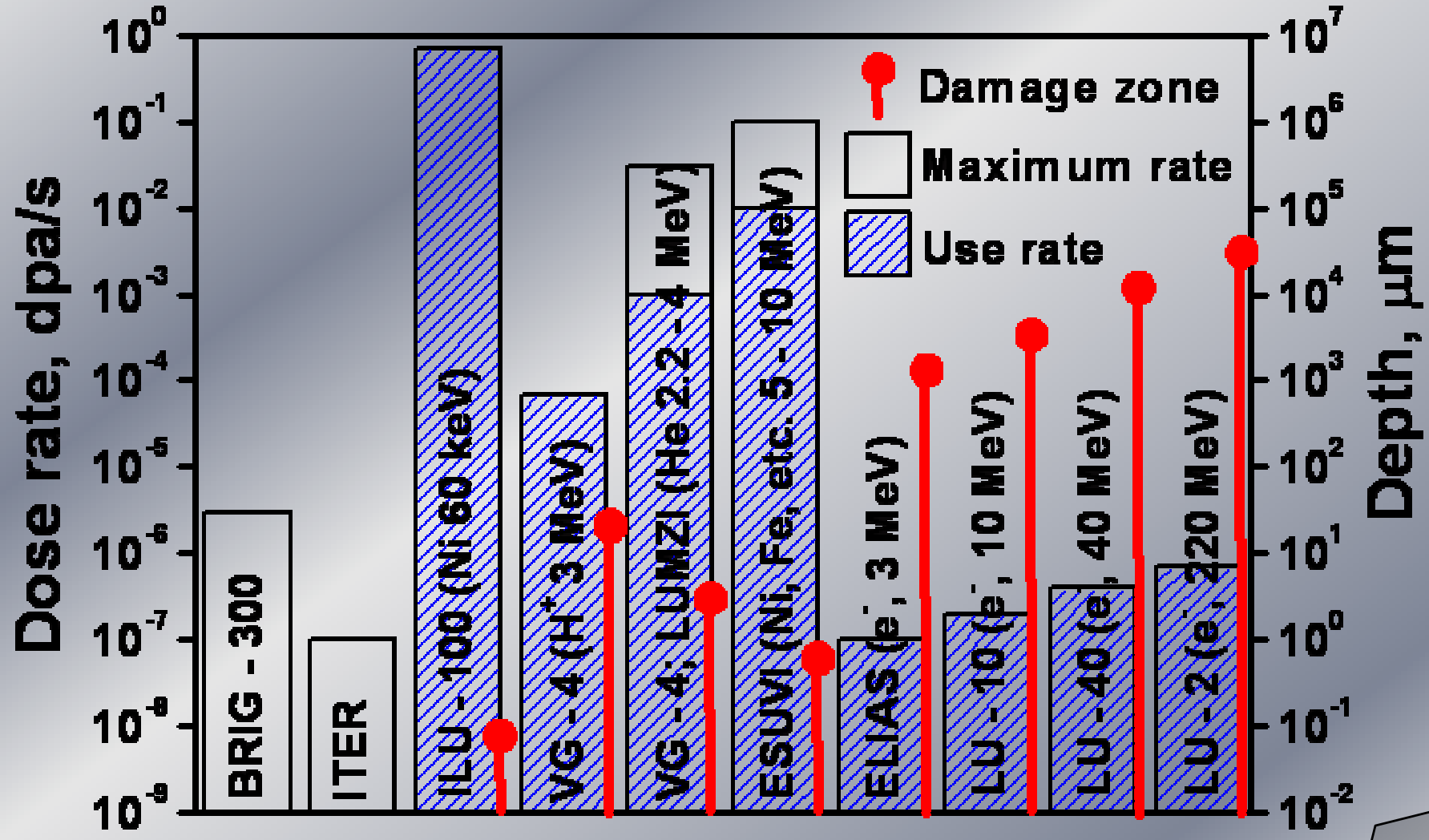

Electrons	Light ions	Heavy ions
➢High dose rate	➢Moderate dose rate	➢Very limited depth of penetration
➢No cascades	➢Good depth of penetration	➢Strongly peaked damage profile
➢Insitu analysis (TEM)	➢Flat damage profile over tens of μm	➢High dose rate
	➢Smaller, widely separated cascades	➢Cascade production

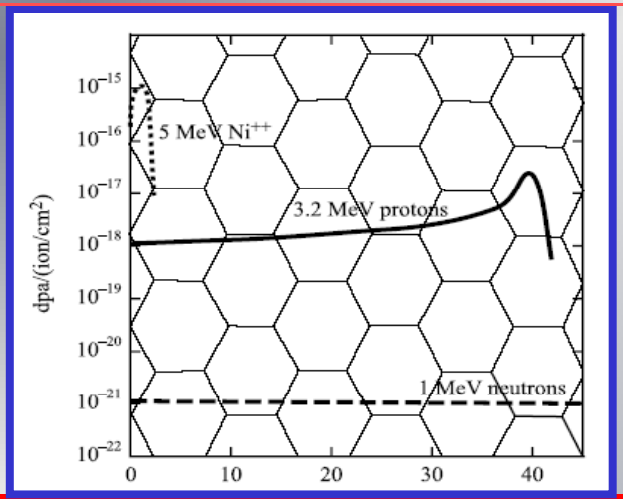

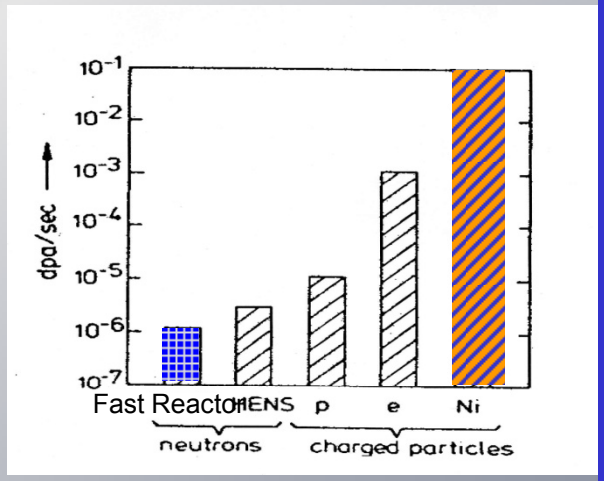

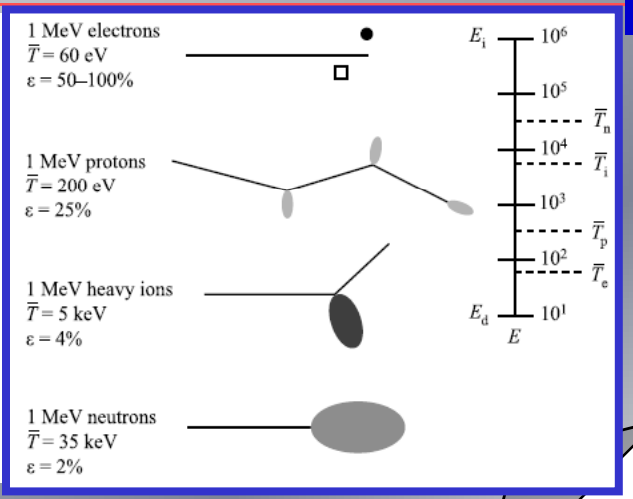

Void Swelling Studies :5MeV Nickel Ions

Disadvantages of ion simulation

- Difference in recoil spectra- difference in the structure of primary radiation damage
- Phase stability at high dpa rate changing of typical for reactor experiment conditions for nucleation and growth of loops and voids
- Injected interstitial effect leads for typical in simulation experiments decreasing of void size
- Stress induced by irradiation –surface proximity

Microstructure of 16Cr10NiTi steel, irradiation in a)BOR-60 reactor (T_{irr}=480^{0}C , D = 53 сна) b) Cr^{3+} ions (3 MeV) (T_{irr}= 625^{0}C, D = 70 сна

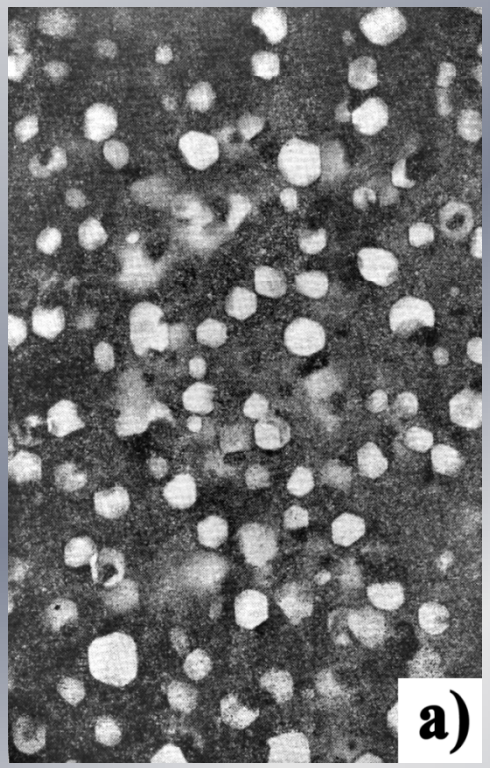

$R_n > R_{ion}$

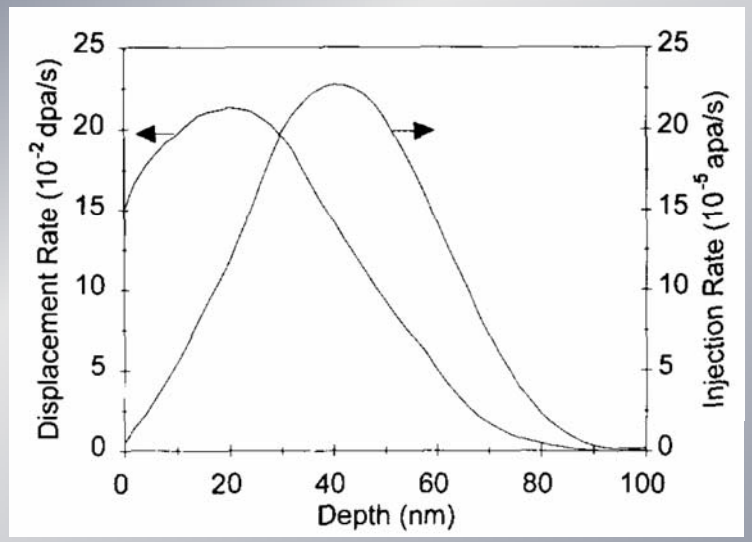

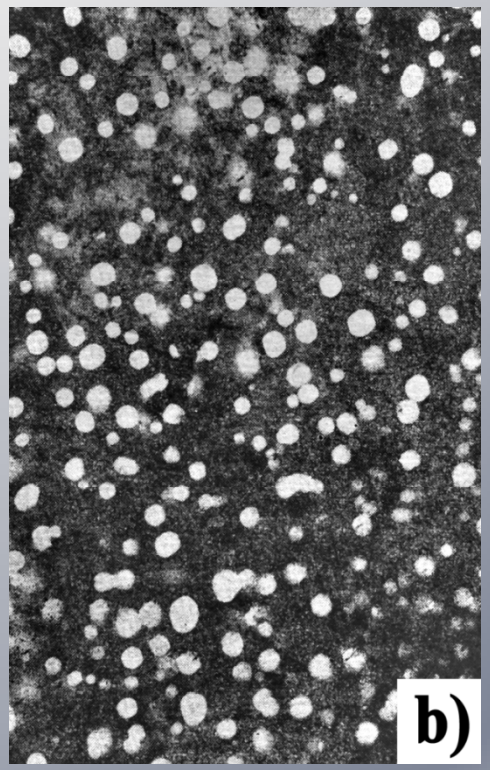

Defect production rate and interstitial injection rate are plotted versus depth for 180 keV Ni^+-ions incident on nickel with a flux of 9.3x10^{17} ions/m^{2}s. Curves were calculated using the TRIM computer code.

Temperature shift

For a given difference in *dose rate*, what difference in *temperature* (at the same dose) is required to cause the same number of defects to be absorbed at sinks?

Main tasks of simulation experiments:

- Investigation of fundamental processes (Simulation of particle collisions, Quantification of kinetic properties of radiation defects, Simulation of formation & growth of defects, defect characteristics depending on radiation dose (type, size, density, etc.)
- R&D materials for fast reactors (swelling and embrittlement) Observation of radiation-induced microstructure such as segregation and hardening
- Microstructural predicting for possibilities of Life extension for exploitating reactors; RPV steels (dpa rate), RVI (low temperature embrittlement)
- Gases influence on mechanisms of radiation damage,Synergetic effect of helium and hydrogen in fusion and spallation systems.

Subcascades in irradiated metals:

a) structure of high energy branches of 100 kV cascade in α-Fe, obtained by dynamic method; numbers-energy of knocked-on atoms, eV; → - direction of their movement;

b) electron-microscopic picture of subcascades in Cu, irradiated by ions of Ar (E=443 MeV)(V.Voyevodin, G.Szenesh,1991)

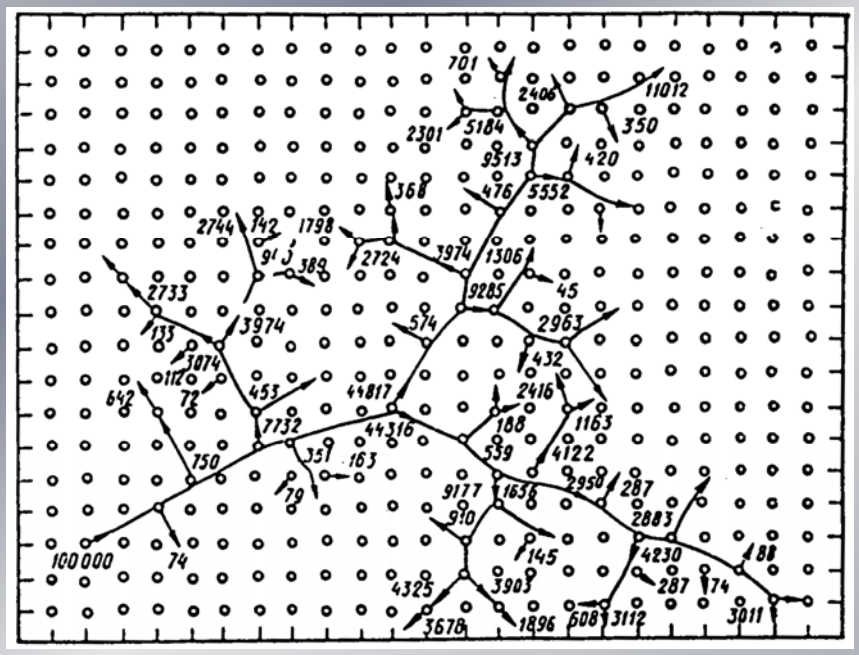

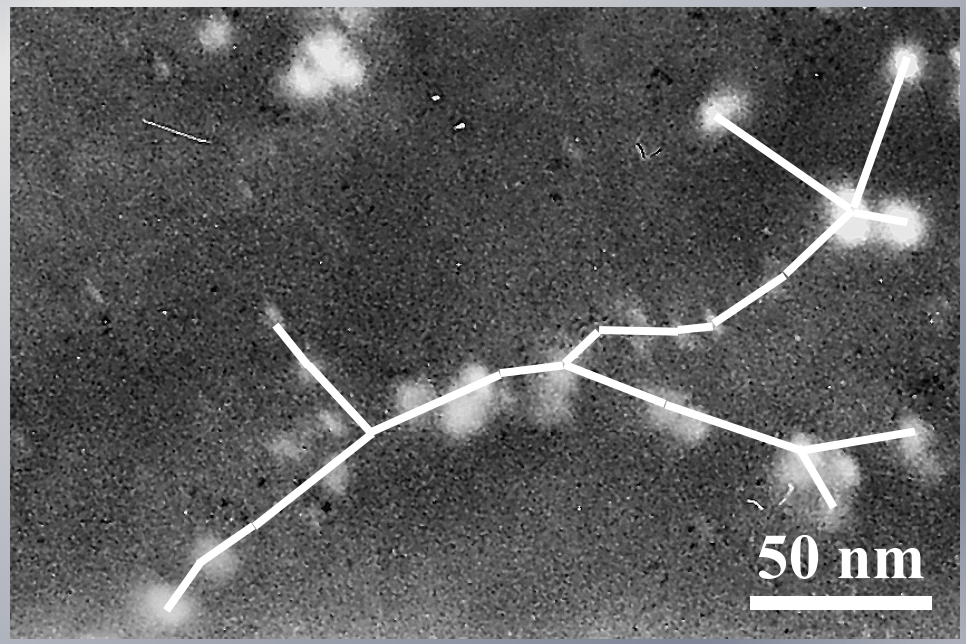

Spectra of isochron annealing of Zr and alloy Zr-Y irradiated by electrons with energy 2 MeV at temperature 82K to fluence $1{,}4.10^{19}$ e^-/cm^2 (V. Borisenko, 2009)

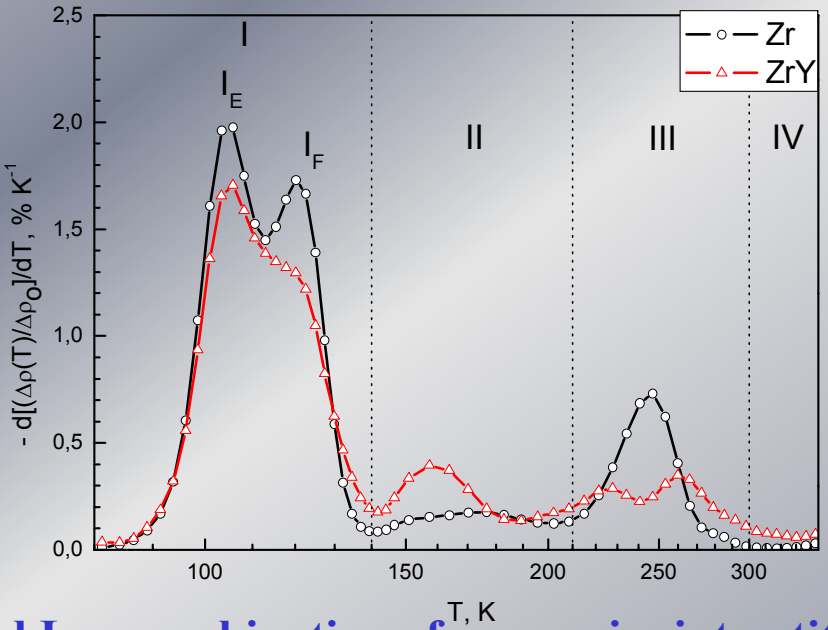

On substages IA, IB and Ic recombination of near pairs interstitial-vacancy occurs

Annealing in zirconium on substages I and IF occurs at the expense of free migration of interstitials

On stage II processes caused by release of interstitial atoms from impurity traps are observed.

According to the one-interstitial model the annealing on stage III is due to the free migration of vacancies.

RADIATION INFLUENCE ON MECHANICAL PROPERTIES IN NICKEL

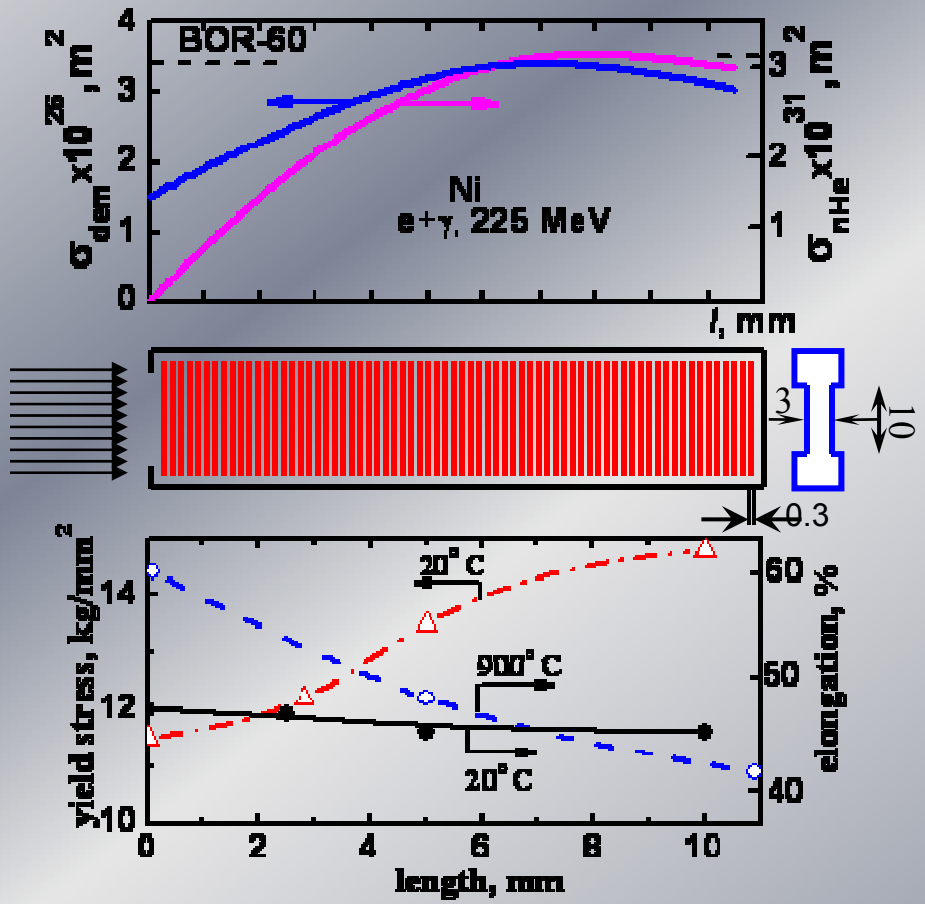

Profiles of primary damages and segregation of helium(a), along the fabrication (b) and evalution of the yelding stress and elongarion (c) in nickel samples, irradiated by electrons and γ-quants with energy 225 MeV

Dependence of nickel elongation versus test's temperature

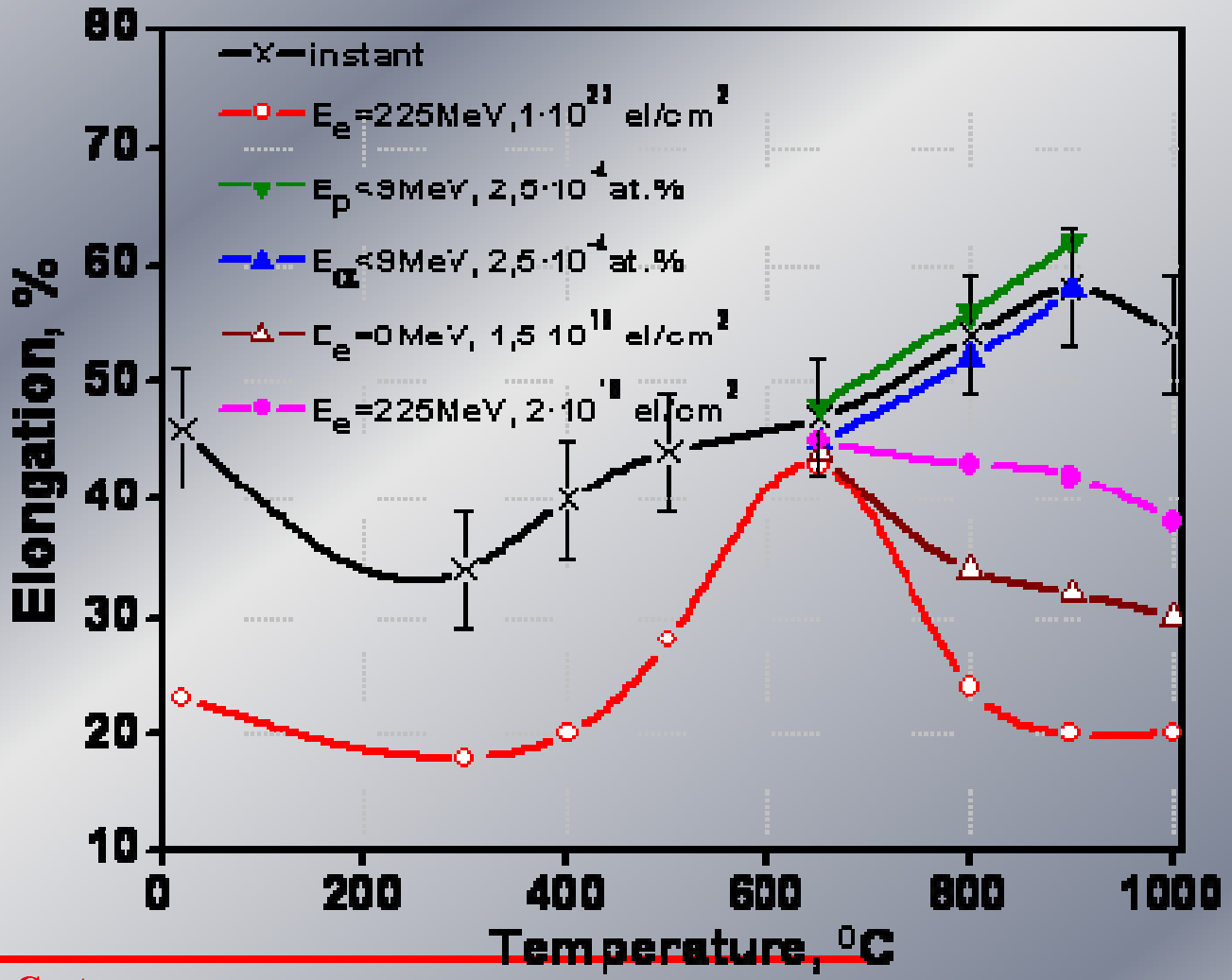

ISOCHRONAL RECOVERY CURVES FOR D9 ALLOYS WITH 0.25% AND 0.15% TI AFTER IRRADIATION WITH 3MeV PROTONS

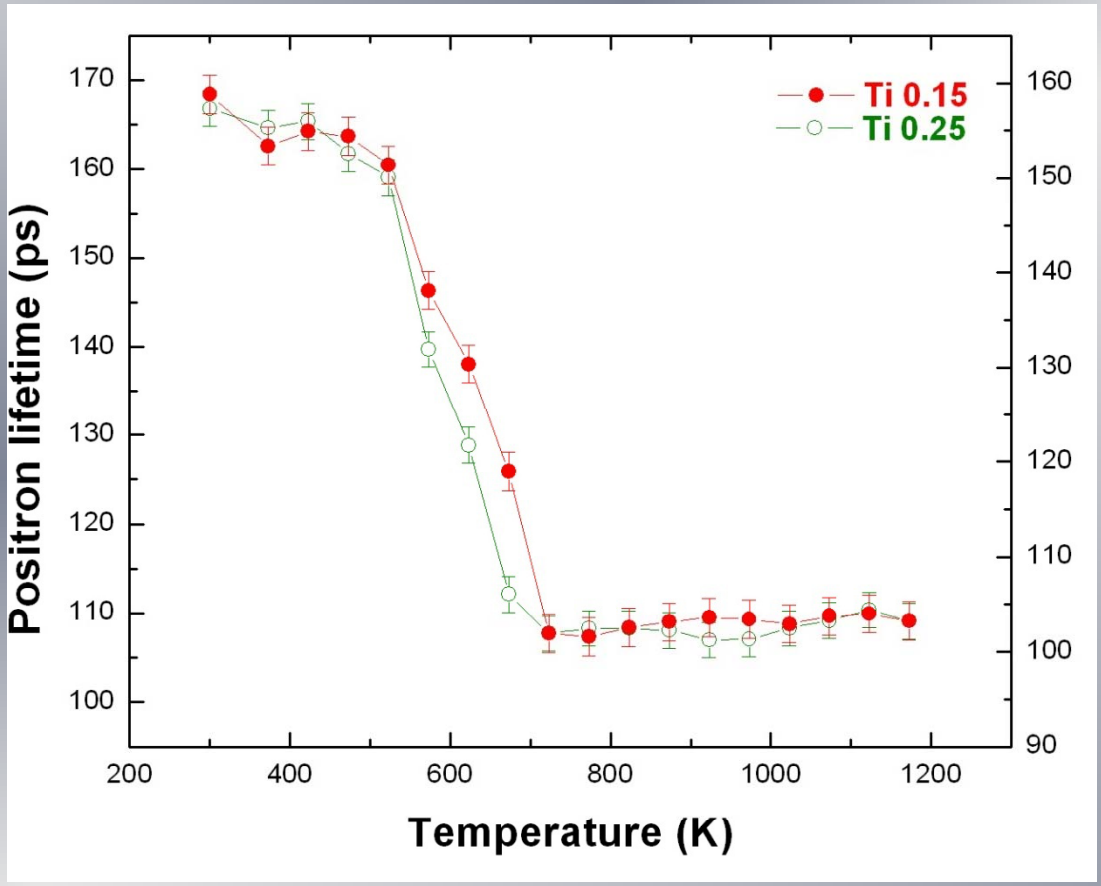

The delayed recovery in the case of alloy with lower Ti suggests slower vacancy migration

Dislocations behavior in A533 steel

A533 (Ni^+ 3MeV, D=1 dpa, T=290^{O}C)

Average diameter of loops d=2.5 nm , $\rho=10^{16}$ cm^{-3} [K.Fujii, 2004]

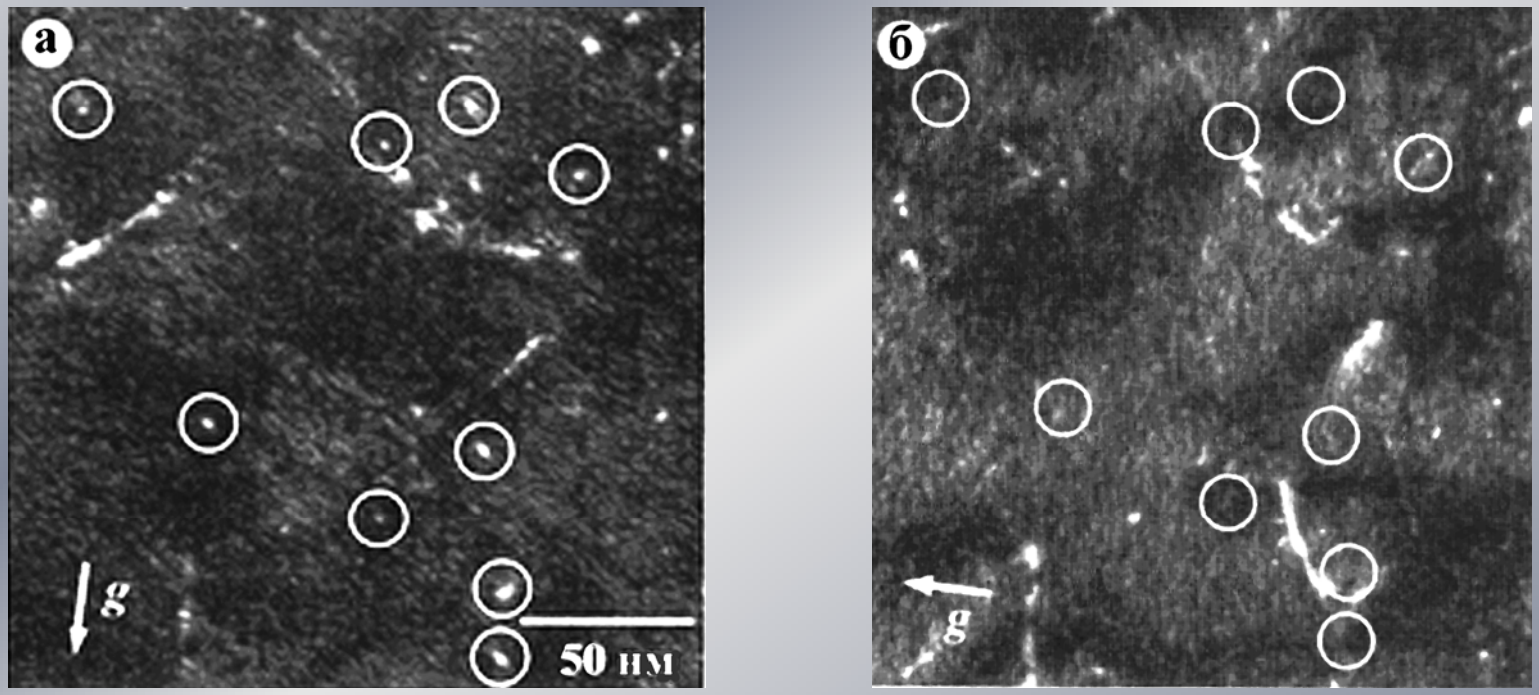

Dislocation loops images in different diffraction conditions : a) g = 020, b) g = 200.

Dislocation loops are visible as white dots. Absence of loops contrast on fig (b) means, that these dislocation loops have Burgers vector b = a<100>.

Dedicated experiments (ion and electron) on low alloyed model alloy (FeCu0.1%)

Copper distribution
(atom probe)

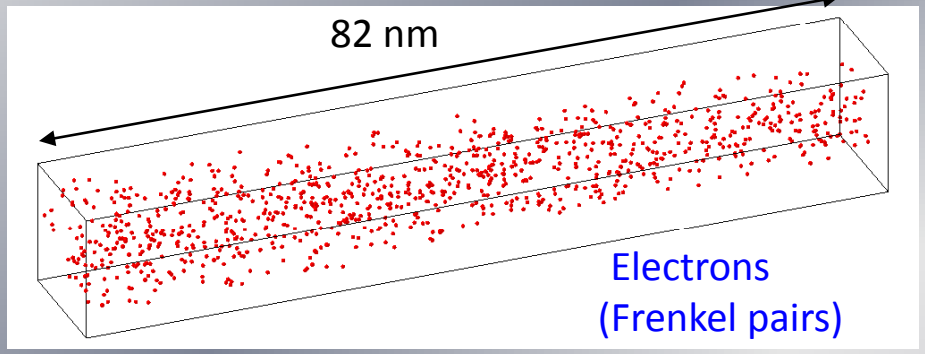

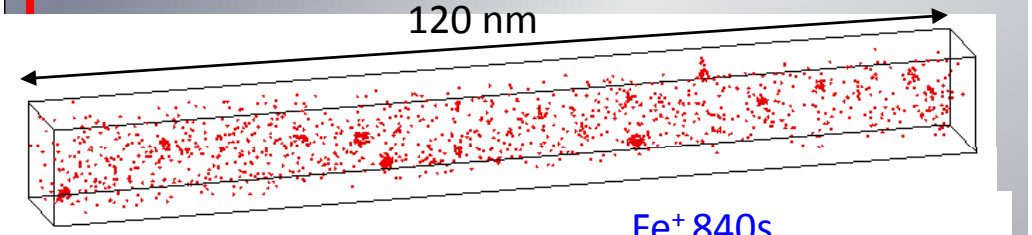

Fe^{+} 840s

(Displacement cascades)

Point defects (MFVIC)

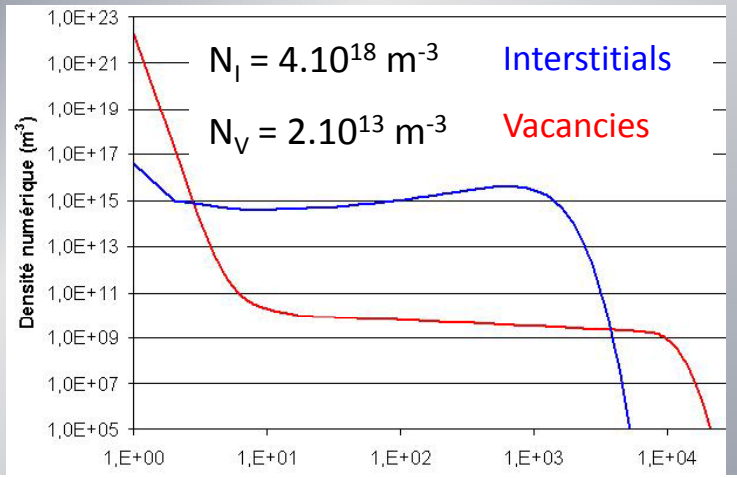

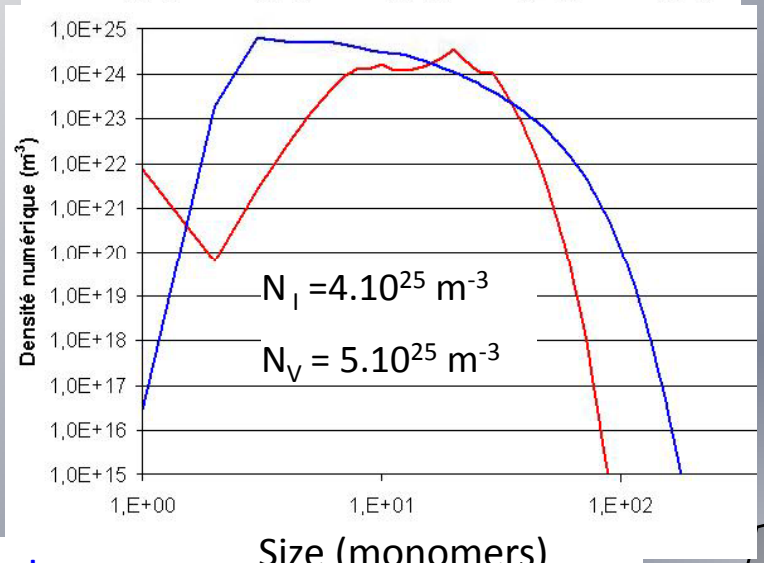

Heterogeneous precipitation on point defect clusters

Dose dependence of hardening for model RPV alloys by neutrons, electrons and proton irradiation all at ~ 300°C

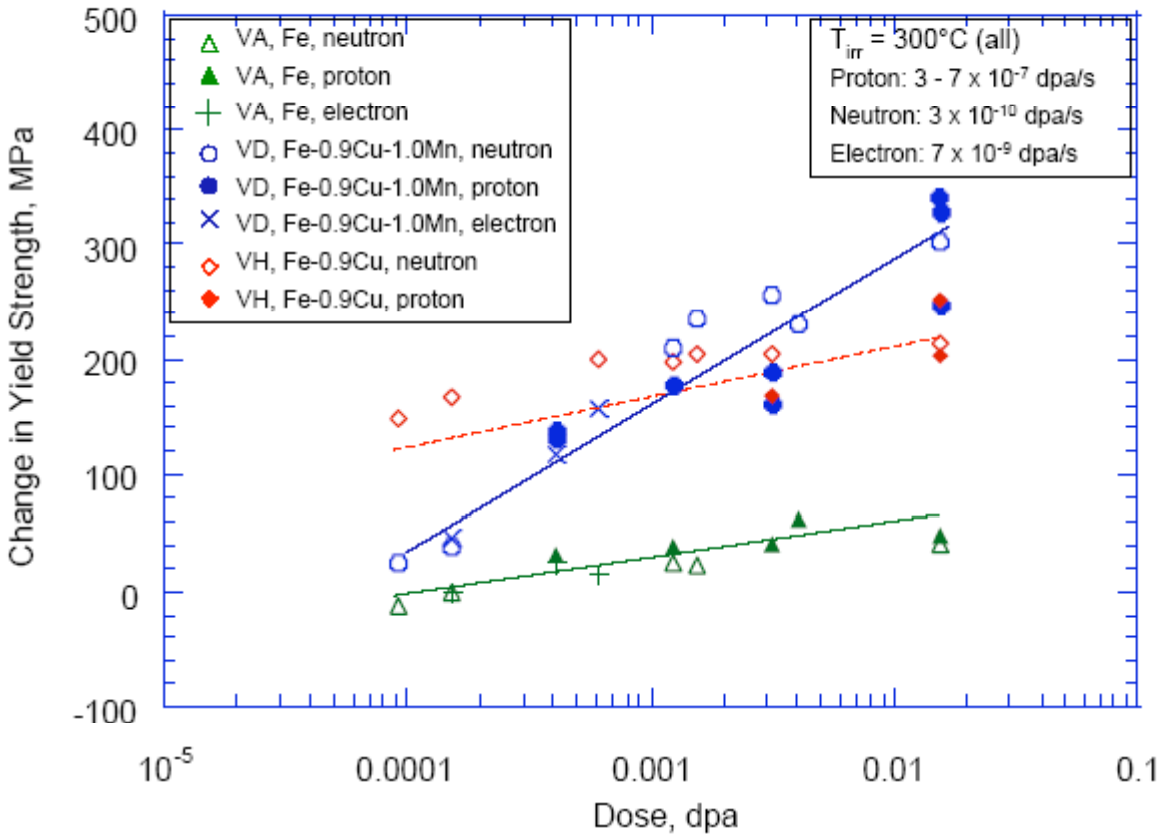

neutrons/electrons: Alexander et al., 9th Env. Deg., TMS, 1999.

Oxygen influence on <c> components dislocation nucleation by ion irradiation

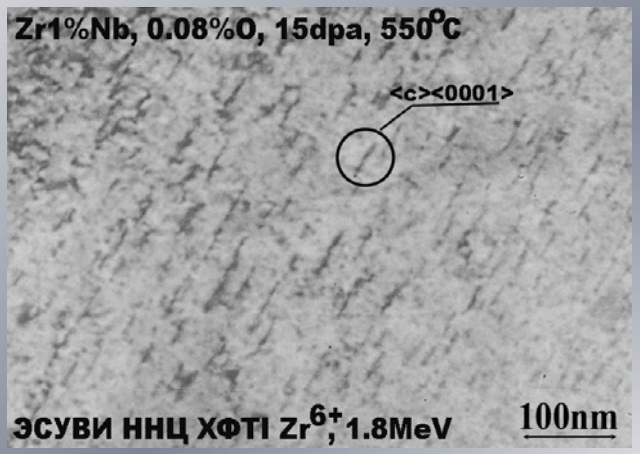

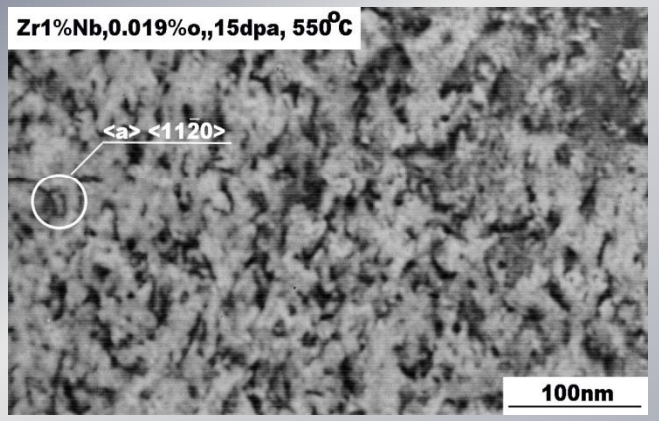

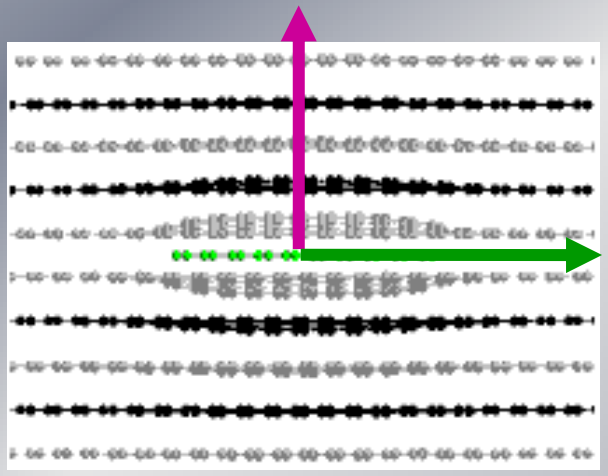

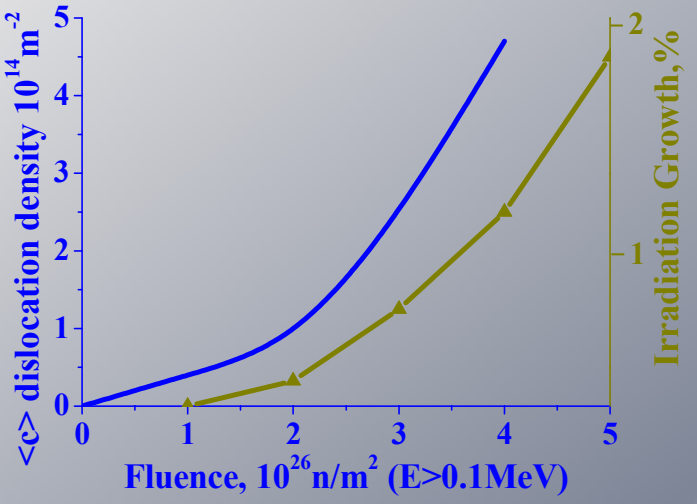

Increase of oxygen content (from 0,08 to 0,2%) in alloy Zr1% Nb causes the suppression of dislocation loops formation of <c> type <0001> being responsible for radiation growth

Parameters of dislocation loops in alloy Zr-1%Nb with different oxygen content (Zr^{6+}, E=1.8MeV, T_{irr}=550°C)

Oxygen contents, % mass	Size of loops, nm		
	Dose, dpa		
	1	10	15
0.08	circular 19,6nm	circular 23,4 nm	circular 24.1nm elongated 48.1
0.14	circular 18.8nm	circular 20.5 nm	circular 22nm elongated 41.6
0.19	circular 13nm	circular 19 nm	circular 21nm elongated-absent!!!

Growth of Hydride (H. Abe, 2007)

Example of growth process of intra-granular hydride（ B=[0001], g = 1010

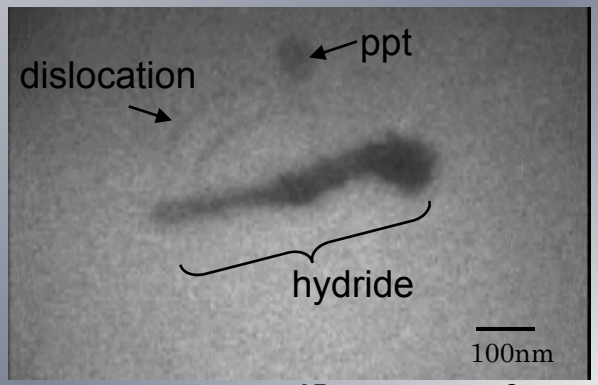

(a)1.5×10^{15} ions/cm^2

(b)2.8×10^{15} ions/cm^2

(c)4.0×10^{15} ions/cm^2

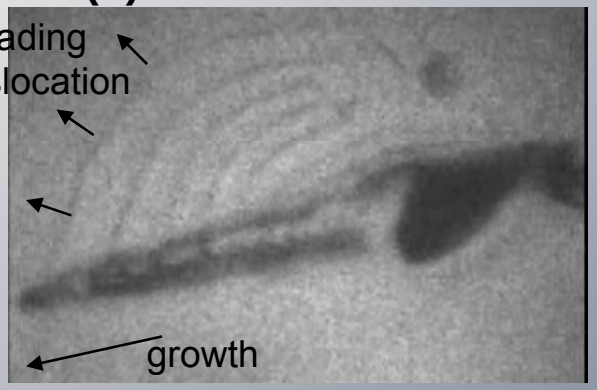

(d)4.8×10^{15} ions/cm^2

Hydrides grew along a specific direction(<1120>) under implantation.
Dislocations were formed associated with hydride growth.
This is the first report on a microscopic evolution of Zr hydride.

Single and sequential beam experiments for ODS: *the underlying metal physics of ferritic steels(M.Fluss,2008)*

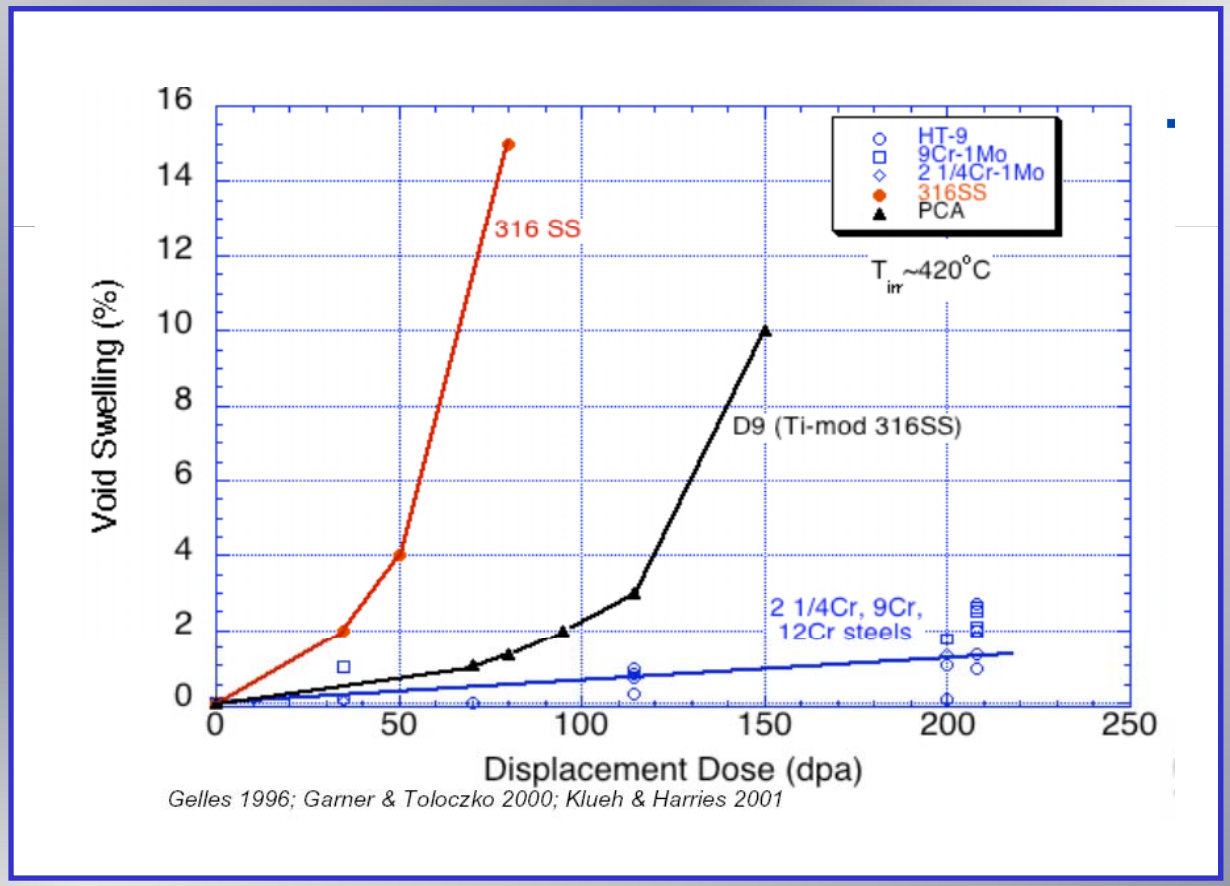

Gelles 1996; Garner & Toloczko 2000; Klueh & Harries 2001

Ferritic steels have better swelling resistance than austenitic steels:

SCIENCE QUESTIONS:

- What structures determine the “intrinsic” incubation time in ferritic steel?
- How do the dispersed oxide phases in ODS “extend” this incubation dose?
- What is the best we can expect from ODS in a fast reactor spectrum like UDB*f-f?*

Acceleration of ion-induced swelling by helium co-injection (Kato et al., 2003)

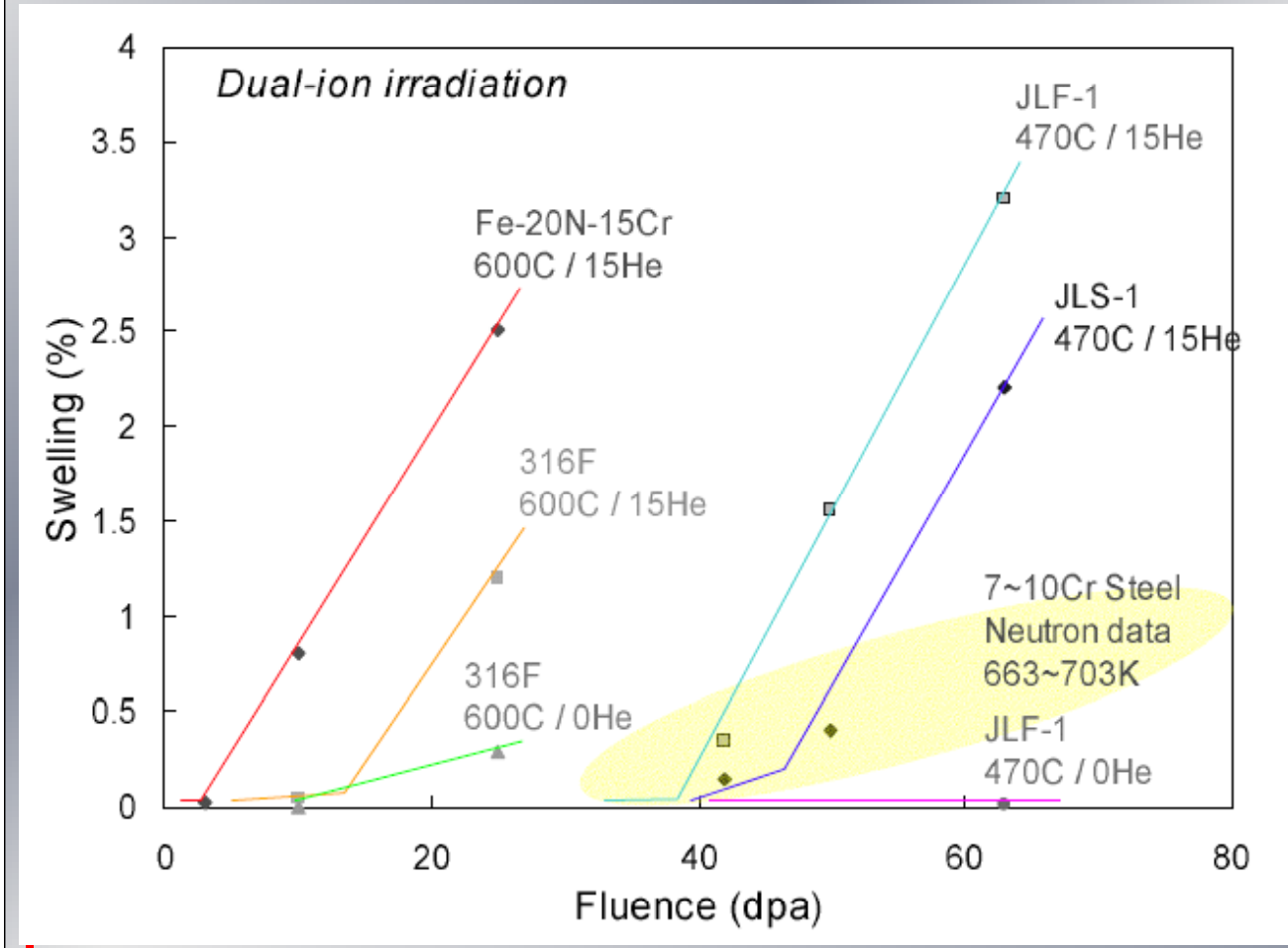

JLF-1 and JLS-2 are Japanese low activation 9Cr-2W ferritic/martensitic steels

6.4 MeV Fe^{3+}

Energy-degraded 1.0 MeV He beam

15 appm He/dpa

Note strong acceleration of swelling in F/M alloys by helium co-injection.

Stages of evolution of dislocation structure in irradiated steel EI-847 (Cr^{3+}, E= 3MeV, T_{irr}=650°C, k=10^{-3}dpa/s): a) D=0,5 dpa; b) D=2 dpa; c) D=10 dpa; d) D=15 dpa; e) D=25 dpa

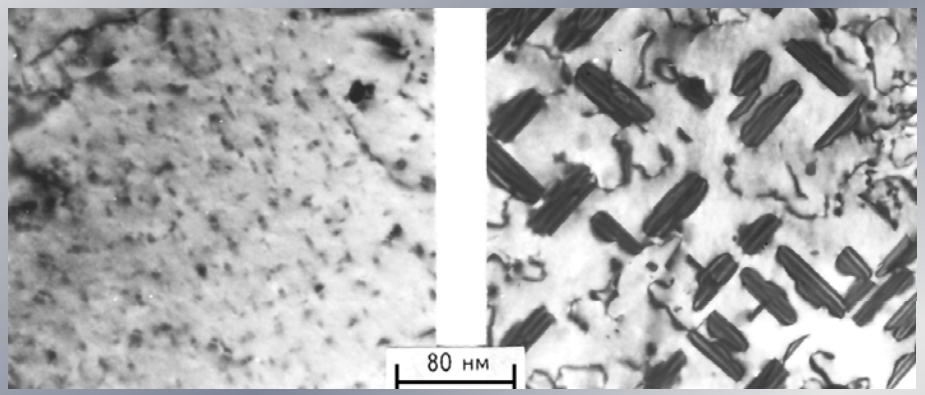

a/3<111> + a/6<11$\bar{2}$> = a/2<110>

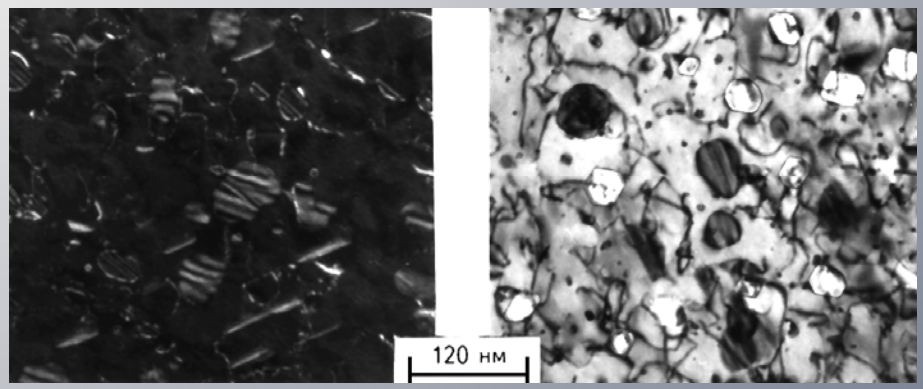

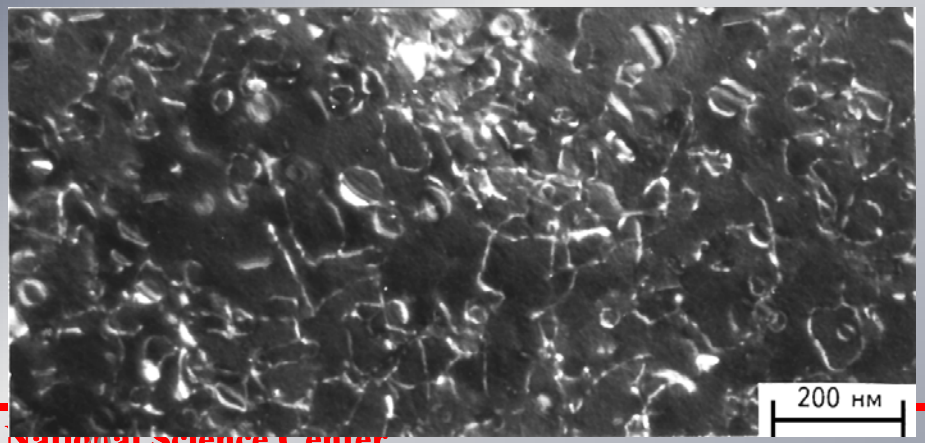

Temperature-displacement rate relationship in RIS for various particle types

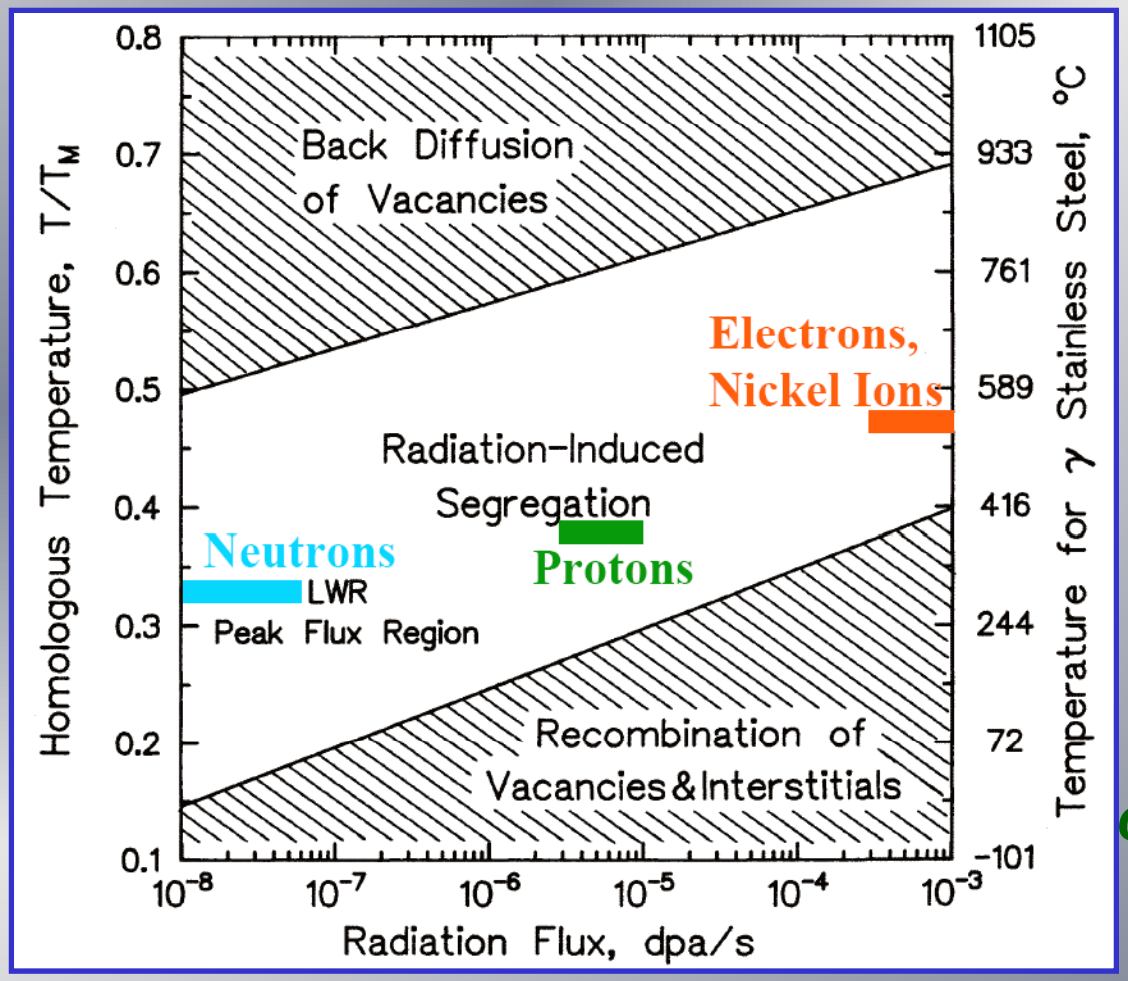

G.Was,2005

Distribution of the elements in defect plate of the Frank loops (dash lines shows average content elements in the matrix): 1– Cr, 2 –Ni, 3 – Si, (EI-847(A), Cr^{3+}, E=3MeV, T_{irr}=600° C, D=25 dpa)

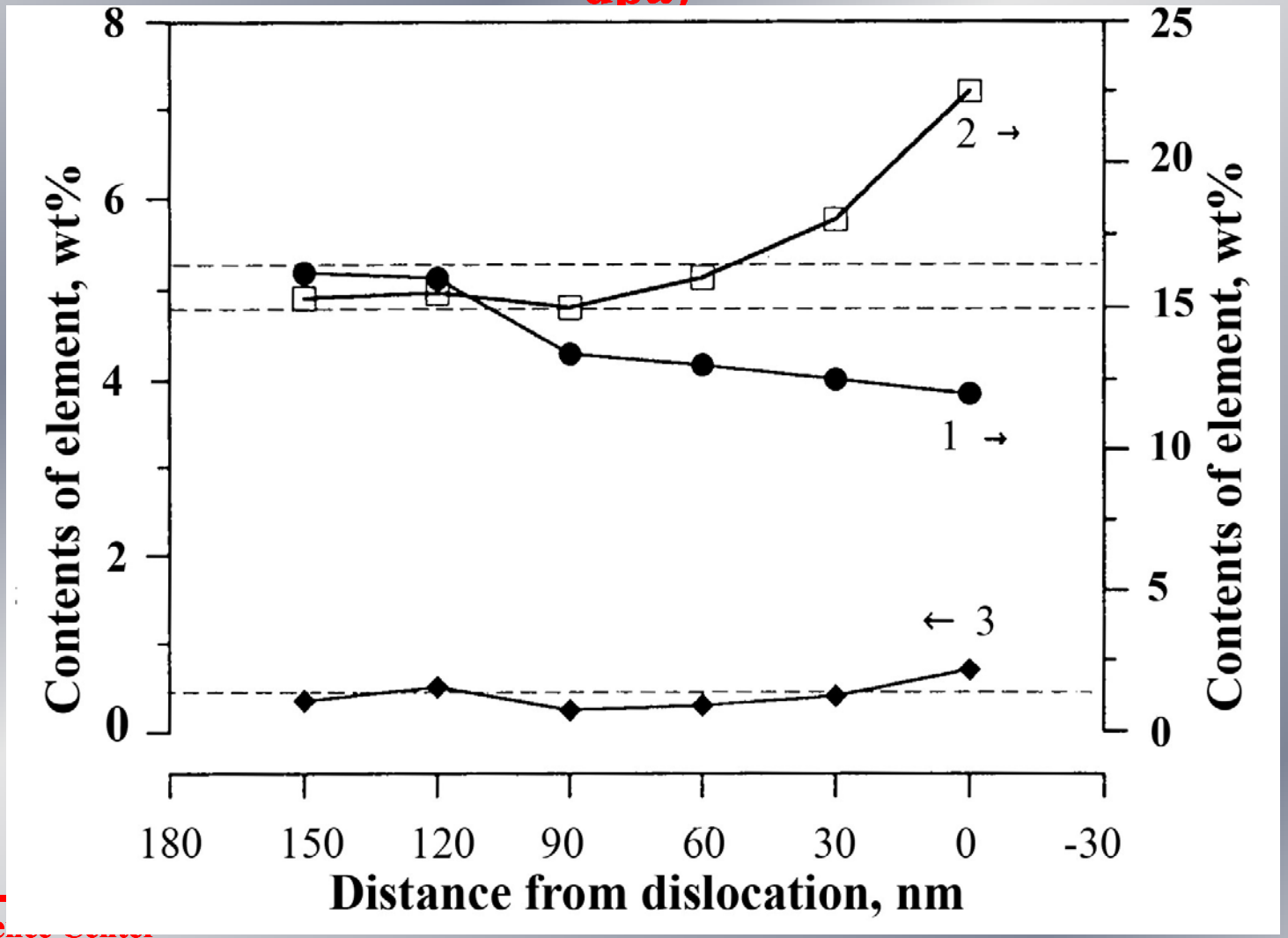

Solute distribution in the vicinity of grain boundary in Fe-Cr-Mn(W,V) alloy (673K/10dpa): a) Irradiation by electron beam (e^-) b) Irradiation by electron/He^+-ion dual-beam (H. Takahashi, 2007)

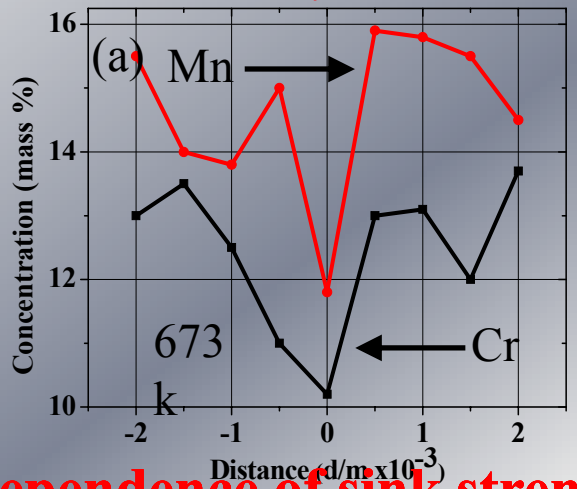

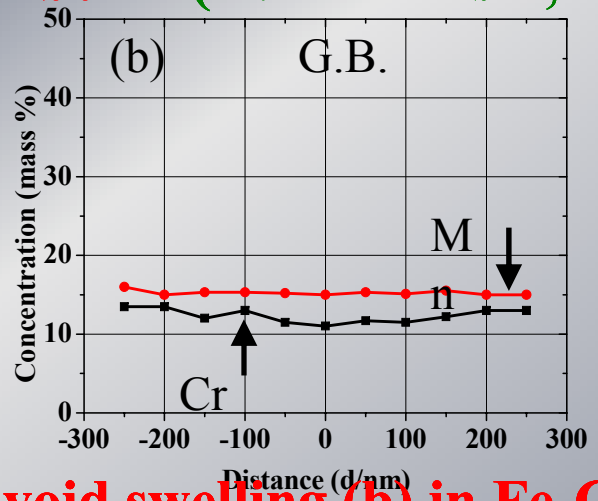

Dose dependence of sink strength (a) and void swelling (b) in Fe-Cr-Mn (W,V) alloy to 10 dpa at 673K

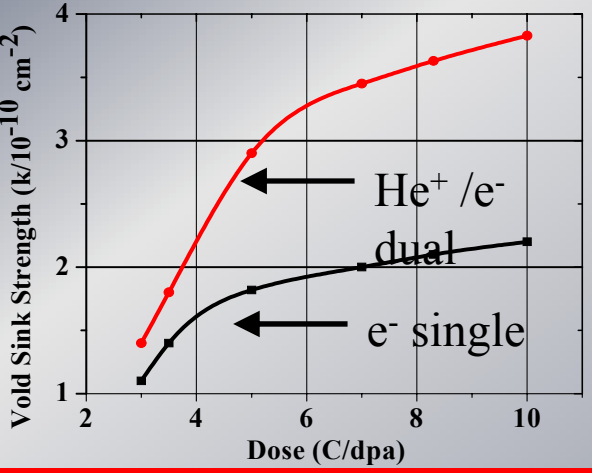

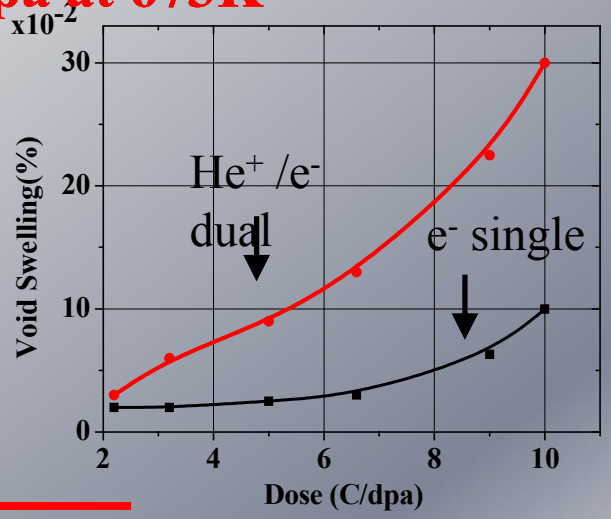

Phase transformation and phase stability

- Nucleation and growth of precipitates with coherent boundaries
- Loss of coherency. Creation on interface sinks of point defects
- Segregation. Elements infiltration from matrix and precipitates on interfaces
- Exceeding of solubility limit. Formation of new precipitates
- More stable precipitates have inerface with higher degree of coherency

Selective segregation on oriented dislocation loop in the 13Cr2Mo ferritic steel (Cr^{3+}, E= 3MeV, T_{irr}= 500°C): a) dislocation loops <100> (D= 15 dpa), b) formation of precipitates (D=52 dpa); c) M2X-precipitate (bid magnification) d) X-ray spectrum from M_2X (X-mainly Cr)

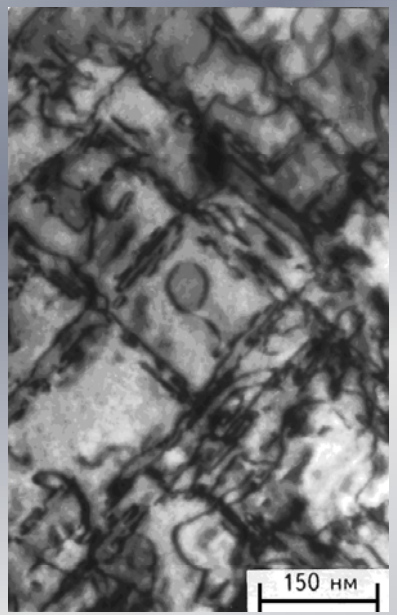

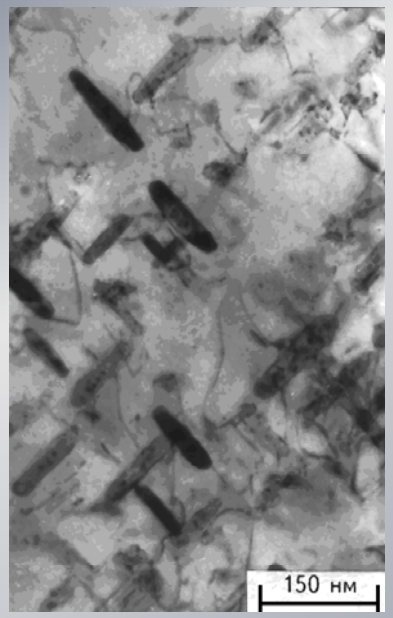

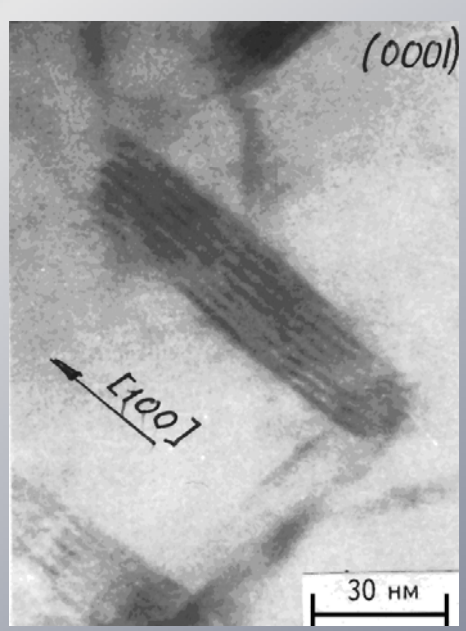

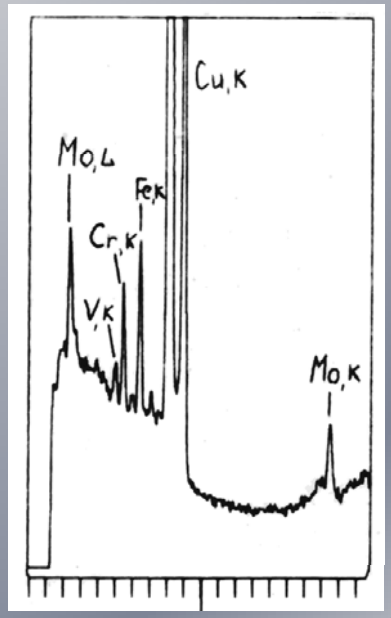

Dose dependence of steel 16Cr-15Ni-3Mo-Nb swelling under electron and Cr-ion irradiation (T_{irr} = 650^{o}C)

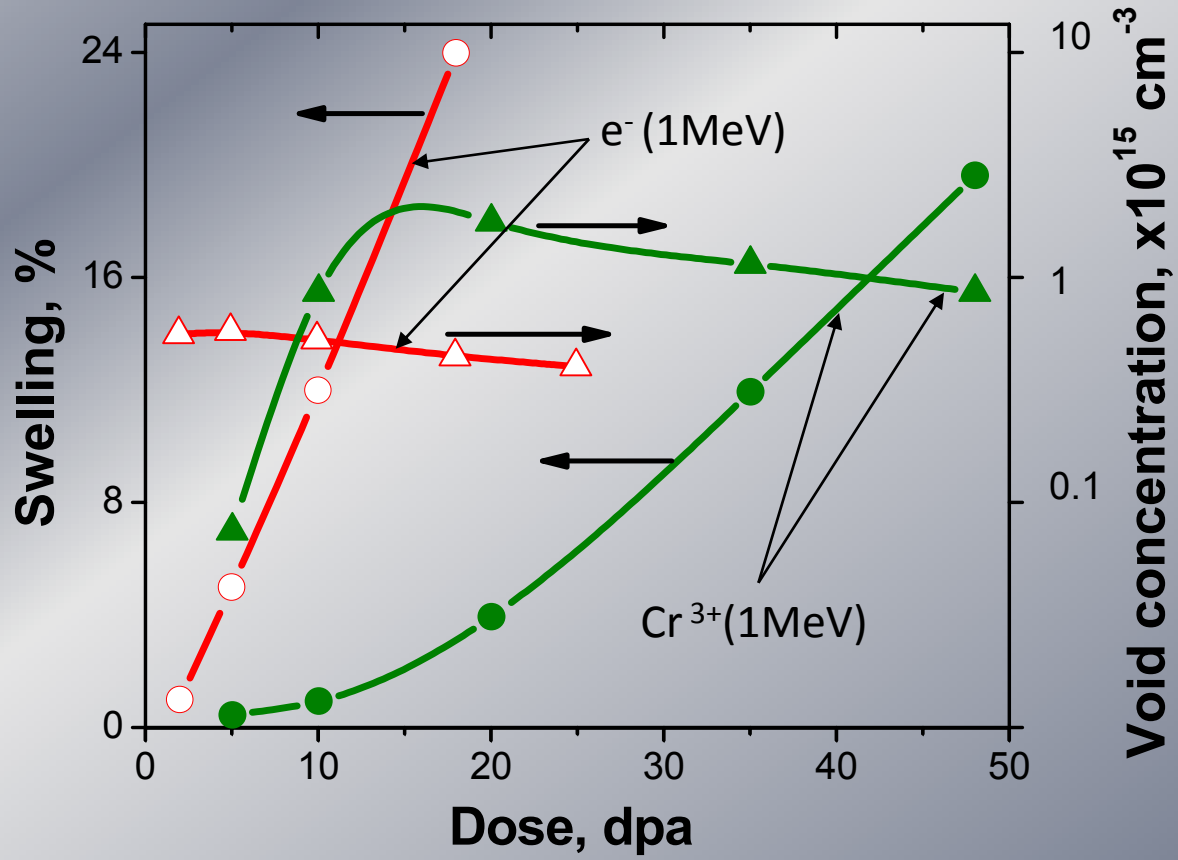

Influence of dpa rate on: a) swelling transient regime (D_0) b) swelling rate ($\dot{S}$) in maximum irradiation temperature

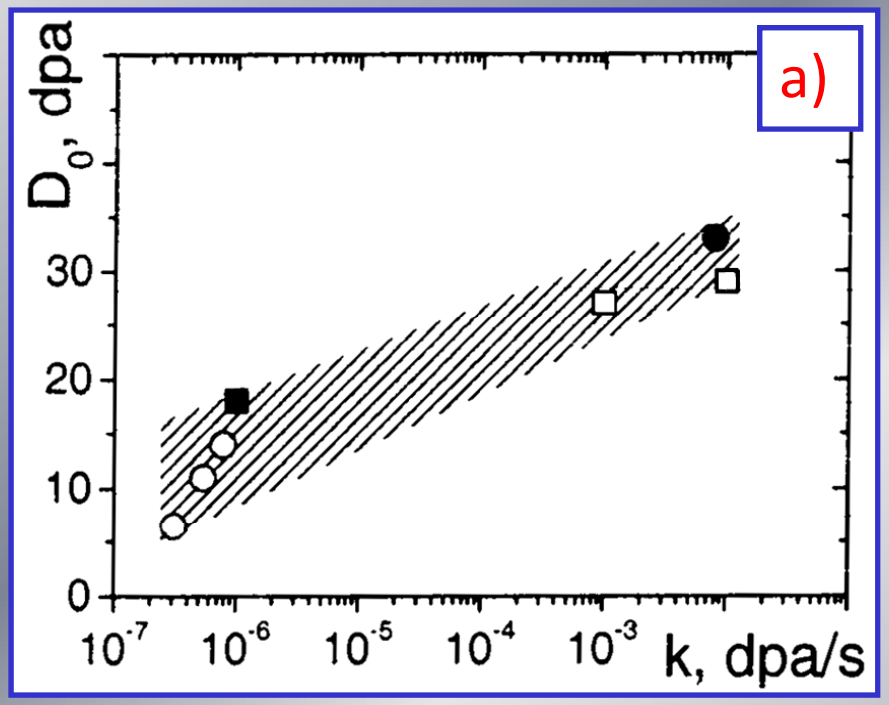

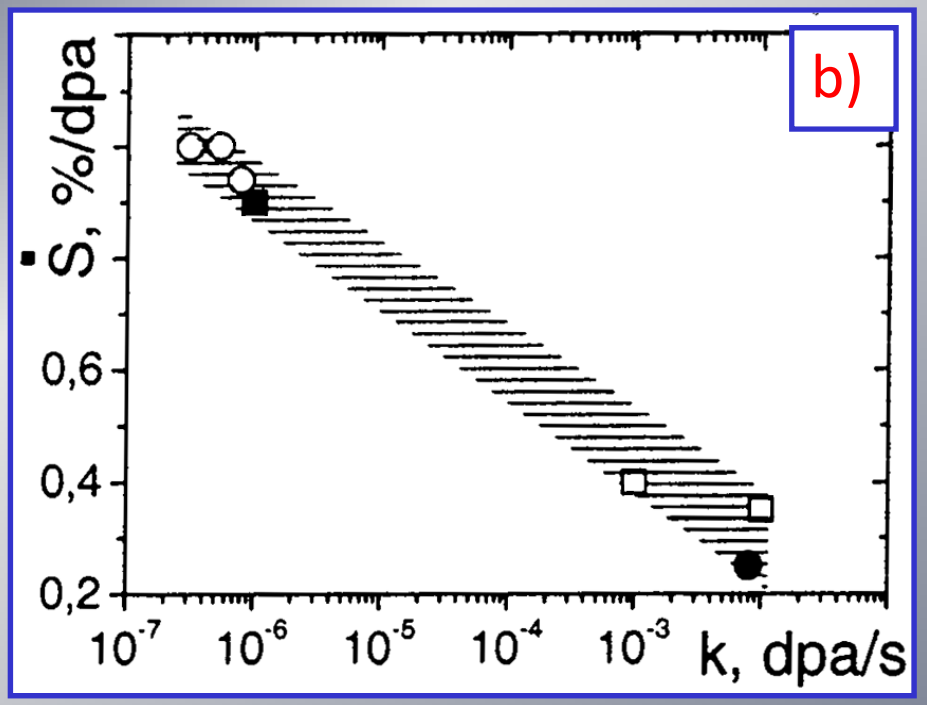

(□) – 18Cr-10Ni-Ti T_{irr} = 615°C and 590°C for 10^{-2} and 10^{-3} dpa/s respectively;
(■) – 18Cr-10Ni-Ti $T_{irr} \approx$ 480°C (BOR-60) [Neustroev V.S. et al, 2000];
(○) – Fe-15Cr-16Ni $T_{irr} \approx$ 410°C (FFTF) [Okita T. et al, 2002];
(●) – 15Cr-16Ni-3Mo-Nb T_{irr} = 650°C (high ions) [Voyevodin V.N. et al].

Temperature and dose rate dependence of swelling of annealed 18Cr-10Ni-Ti at a dose of 50 dpa.

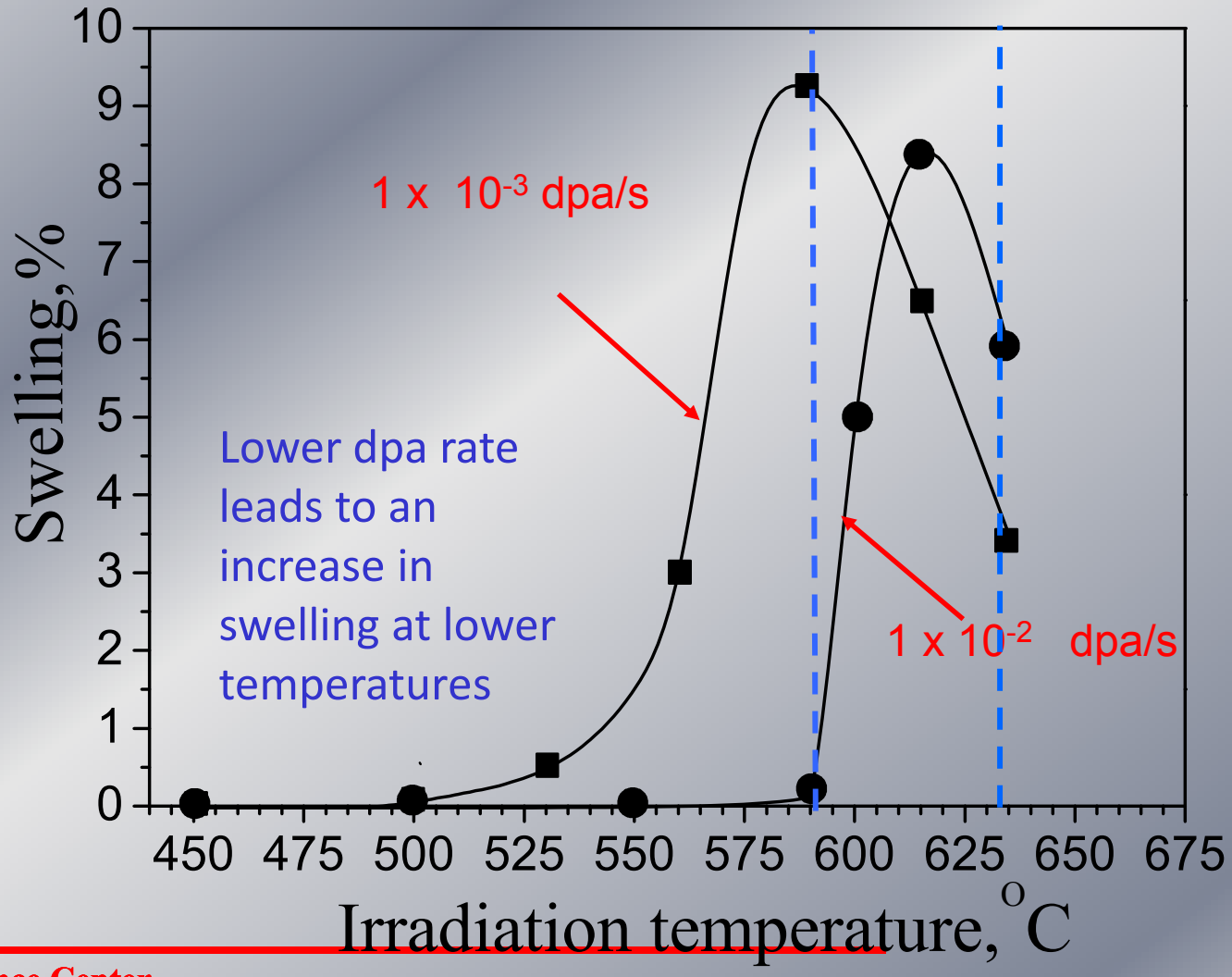

Mechanisms of deuterium retention in steel 18Cr10NiTi on helium bubbles

Steel microstructure development in steel under irradiation by ions of helium and hydrogen and post implantation annealing

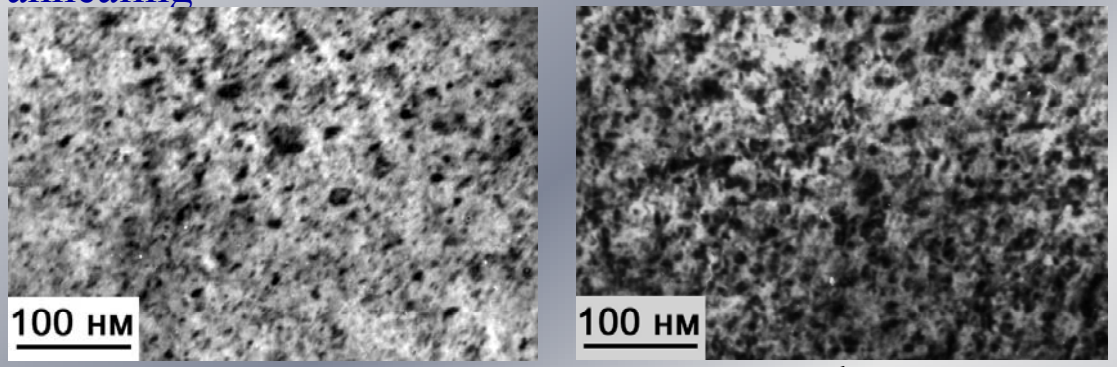

a b

Microstructure of steel 18Cr10NiTi irradiated by helium ions with energy 12 KeV at $T_{irr.}$ up to the dose $5.10^{15}cm^{-2}$ (a) and $5.10^{16}cm^{-2}$ (b)

Helium thermal desorption

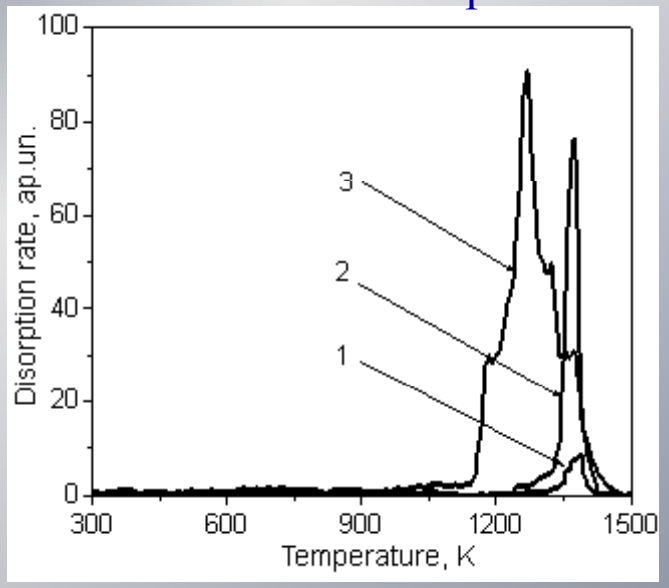

Dose dependence of helium release from steel 18Cr10NiTi irradiated by ions of He^+ at T=290 K up to the doses 5.10^{14} (1), 5.10^{15} (2) and 5.10^{16} (3) ions/cm^2. Rate of heating 4°/s

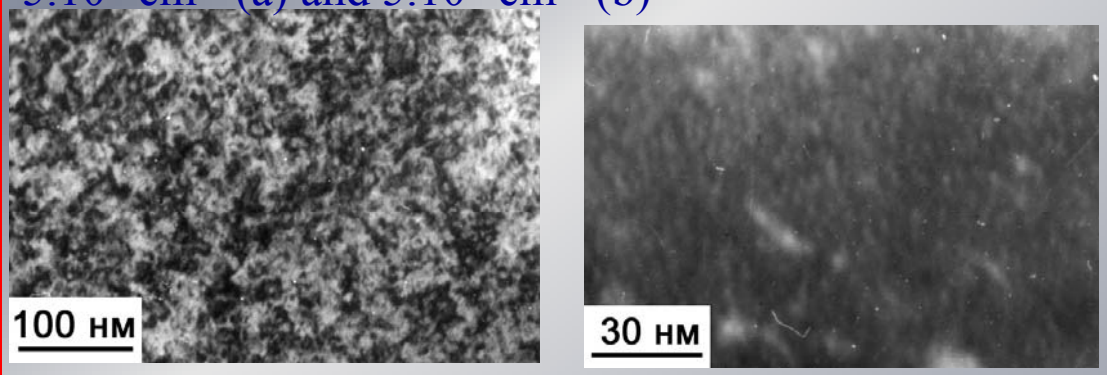

a b

Microstructure of steel 18Cr10NiTi after irradiation at T by helium ions up to the dose $5.10^{15}cm^{-2}$ (a) and $5.10^{16}cm^{-2}$ (b) and by hydrogen ions up to the dose $1.10^{16}cm^{-2}$ and subsequent annealing at 600 K.

Complex synergies call for aggressive exploratory research(M.Fluss,2008)

Swelling of FeCr Model Alloys Fe9Cr Fe12Cr
- Enhanced to ~ 4% for 12Cr alloy.
- Much higher in 9Cr than in 12Cr alloy.

- Fe9Cr and Fe12Cr Alloys
- Single, dual and triple ion-beams : Fe3+, He+ and H+
- 50 dpa at 510° C. TIARA facility
- Accelerating V Fe^{3+}, He^{+} and H^{+}: 10.5 MeV, 1.05 MeV, 380 keV.
  1) single ion (Fe^{3+}) : good swelling resistance (0.5%) for both.
  2) dual ion (Fe^{3+} + He^{+}) of the 12Cr alloy: swelling of 0.4%.
  3) dual ion (Fe^{3+} + H^{+}) : No effect of the presence of H+
  4) triple ion (Fe^{3+} + He^{+} + H^{+}) !!!

- IEA-heat F82H (Fe–8Cr–2W–0.2V–0.04Ta–0.1C) Steel
  - (a) triple beams of Fe^{3+}, He^{+} and H^{+} ions
  - (b) dual beams of Fe^{3+} and He^{+} ion
- 50 dpa, T= 470 °C
- Irradiations TIARA facility JAERI
- Cavities formed in F82H at the depth of ~ 1 μm

The synergistic effect of He and H was shown clearly in the triple ion (Fe^{3+} + He^{+} + H^{+}) irradiation

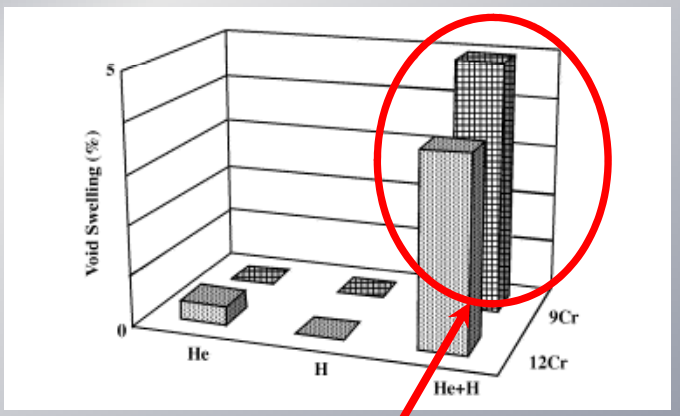

T. Tanaka et al. JNM 329-333(2004)294

The average swelling in F82H steel was significantly enhanced by the triple ion irradiation

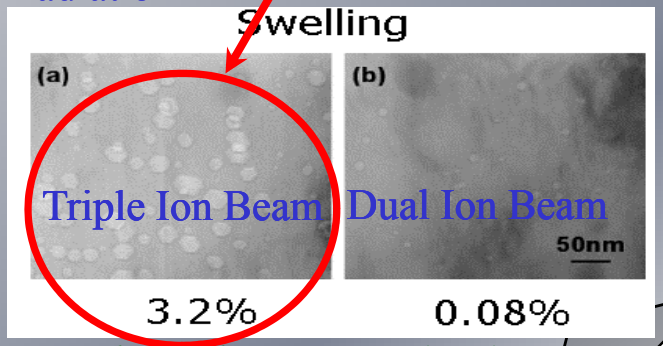

E. Wakai, et al. JNM 307-311(2002)278

Methodological aspects

1. TEM

$$\frac{\Delta V}{V} = 100\% \cdot \frac{\frac{\pi}{6}\sum_{i=1}^{N} d_i^3}{S_A \cdot l_A}$$

2. Step height measurements of void swelling

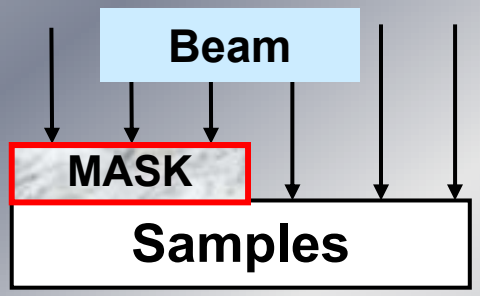

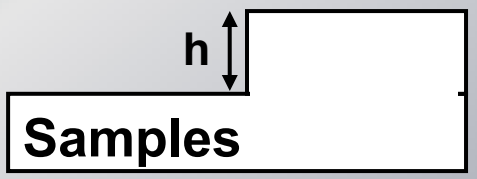

$$h = \frac{S_A}{1 + S_A}\Delta R$$

3. Cross Section

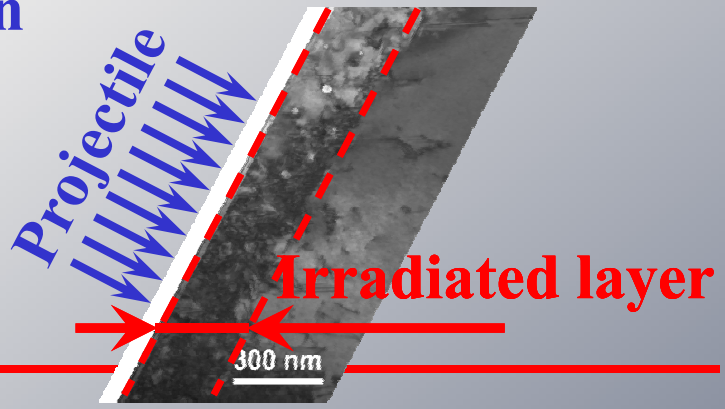

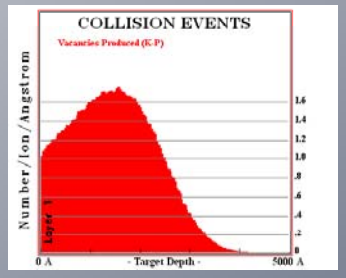

Accelerator ESUVI ion guide and hollow source of gas ions of magnetron type

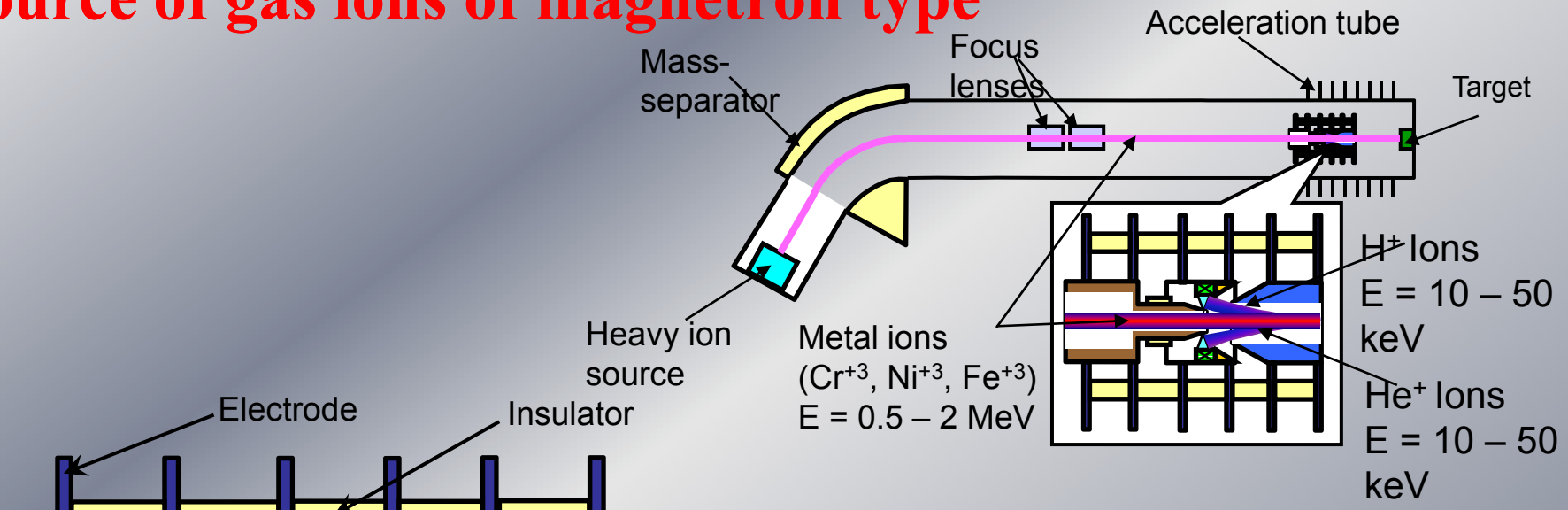

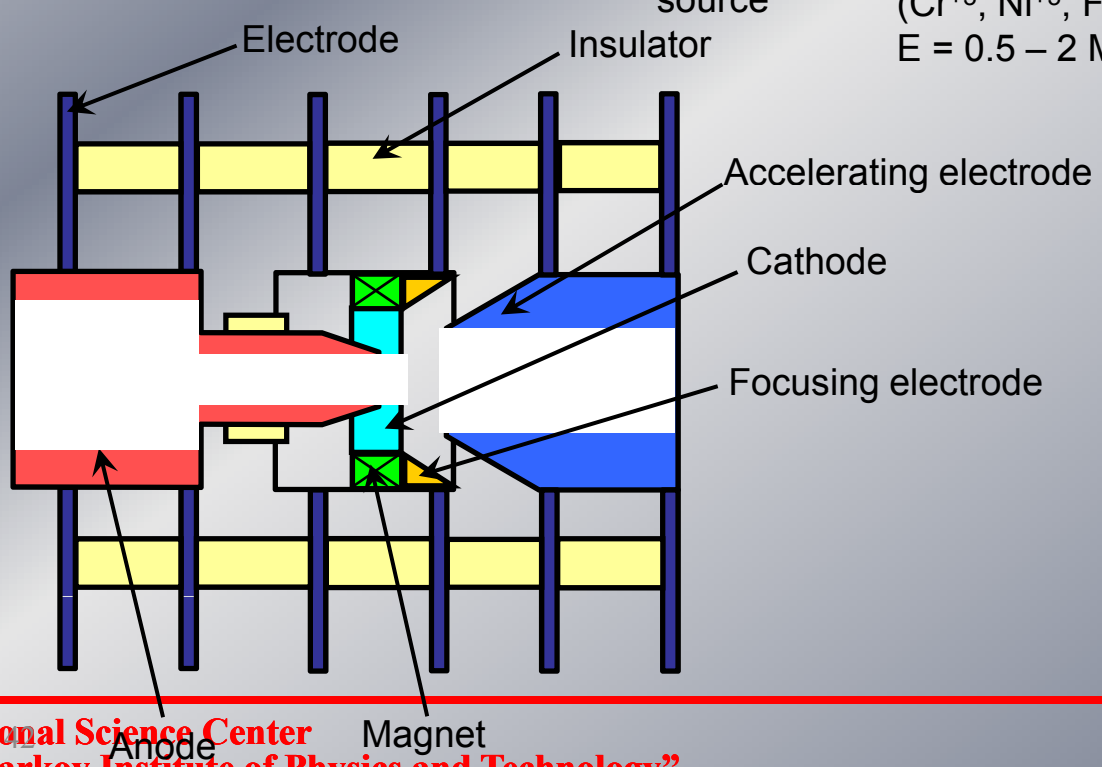

Electrostatic Accelerator with External Injector (ESUVI)

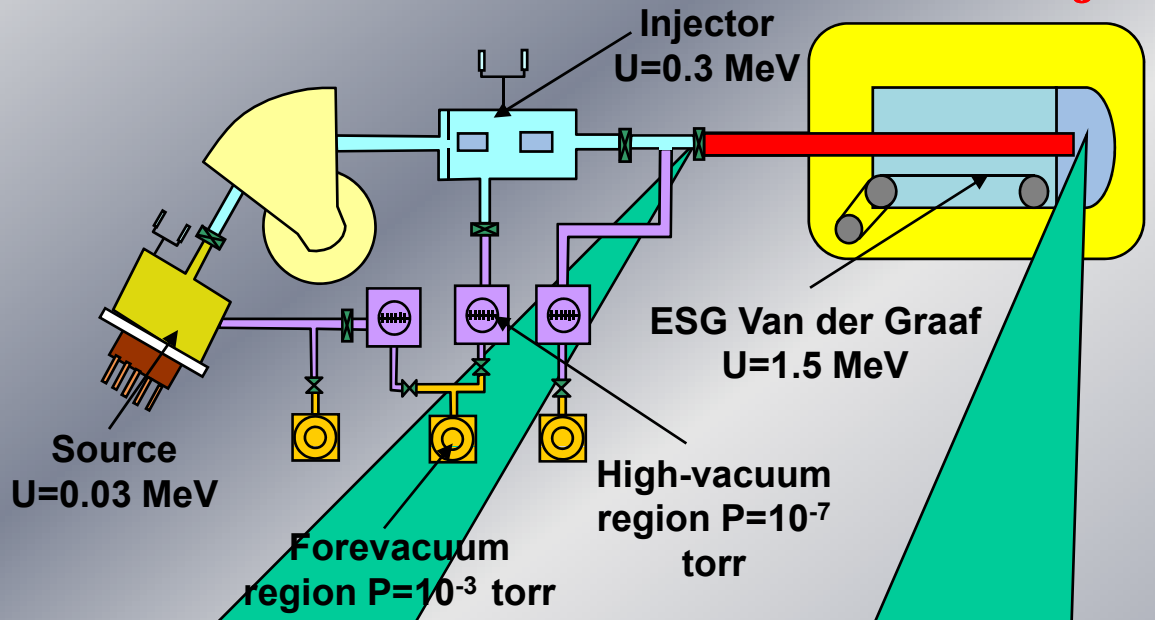

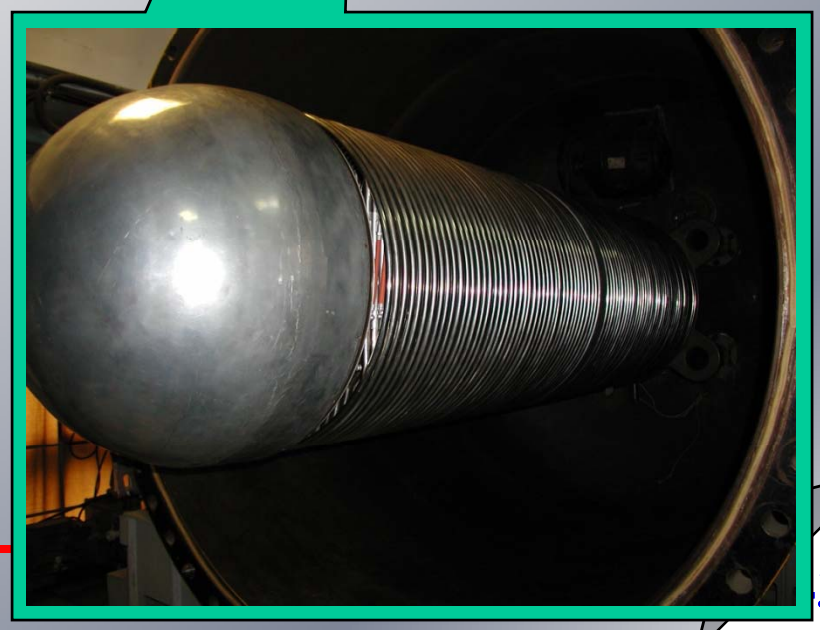

Facility for triple-ion irradiation

(stage of putting into operation)

1-ion source
2-accelerator tube
3-intermediate chamber
4- 85°- magnet
5-vacuum system

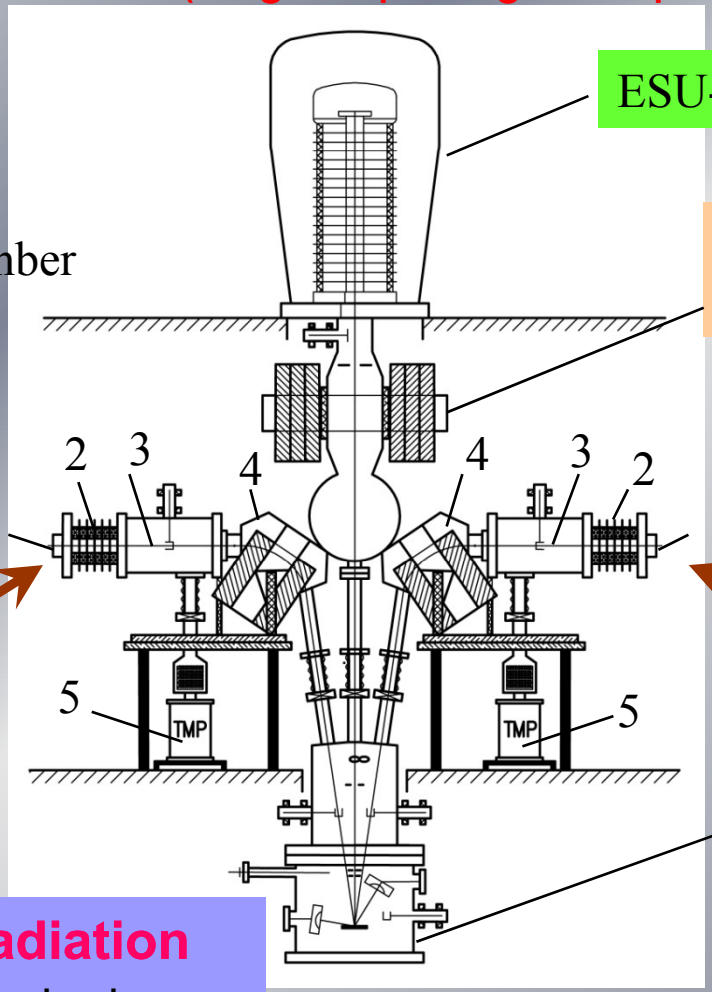

Accelerator of Helium Ion 2-50 keV

Accelerator of Hydrogen Ion 2-50 keV

chamber for irradiation of targets and measurements using the methods of nuclear reactions

Triple-ion irradiation
Damage +helium + hydrogen

Profiles of deuterium and helium

$^3He + D \rightarrow p + {}^4He$

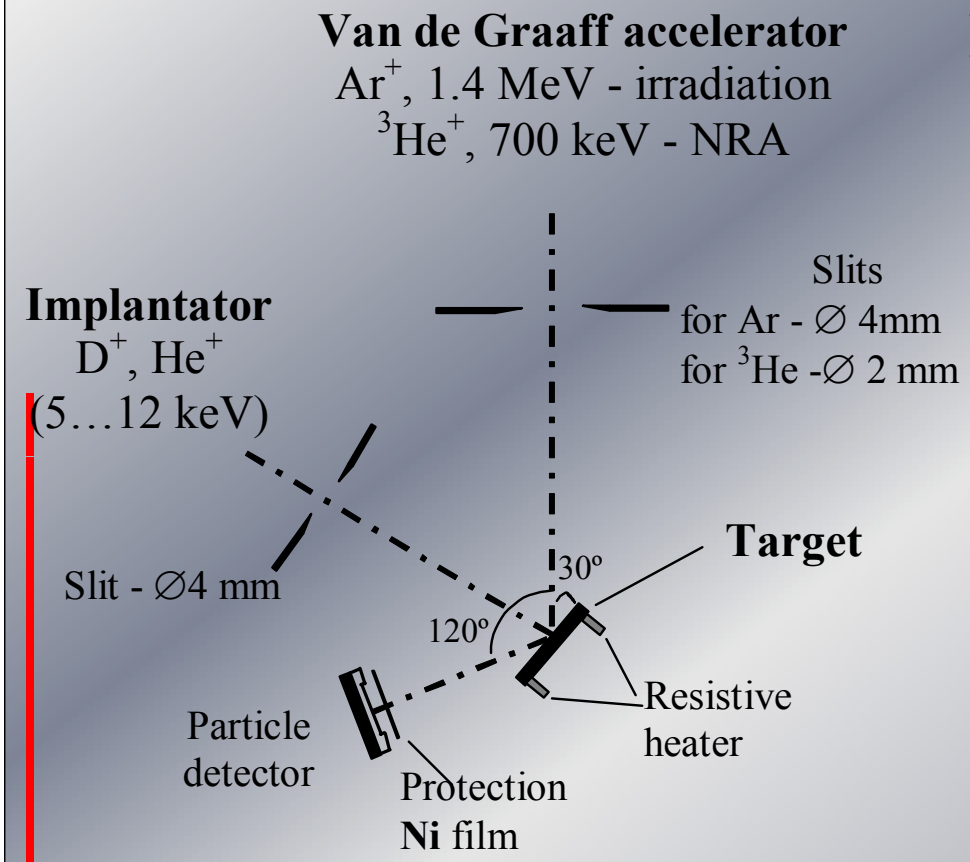

Nuclear reaction analysis

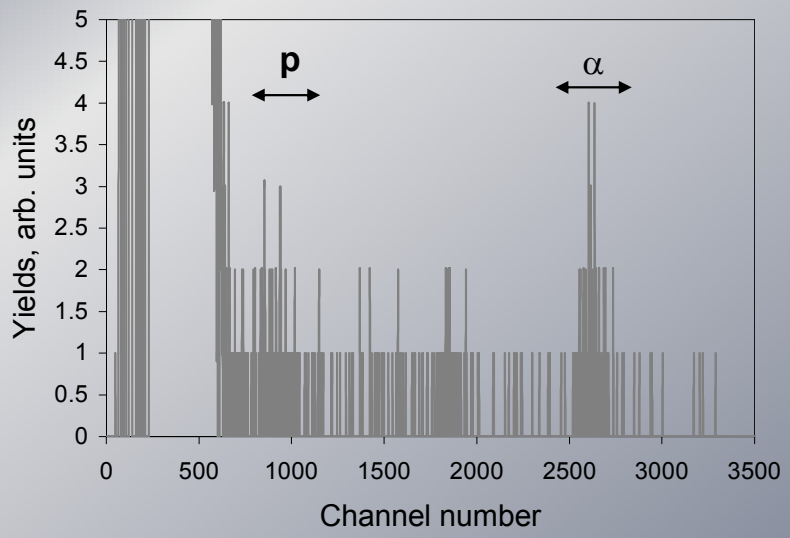

Spectrum of the $D(^3He,p)^4He$ reaction

The sensitivity of Nuclear Reaction Analysis method (NRA) is deteriorated by the presence of large sources of background. To attenuate the back-scattered particle effect a nickel film of 0.5 μm thickness was placed in front of the surface-barrier detector. This leads to energy spectrum broadening of the reaction products.

By varying the argon implantation angle we obtained different levels of damage and concentrations of argon atoms at depth between 0-100 nm

1.4 MeV Ar^+ ($5 \cdot 10^{16} cm^{-2}$) + 5 keV D^+ ($5 \cdot 10^{16} cm^{-2}$) → 18Cr10NiTi SS

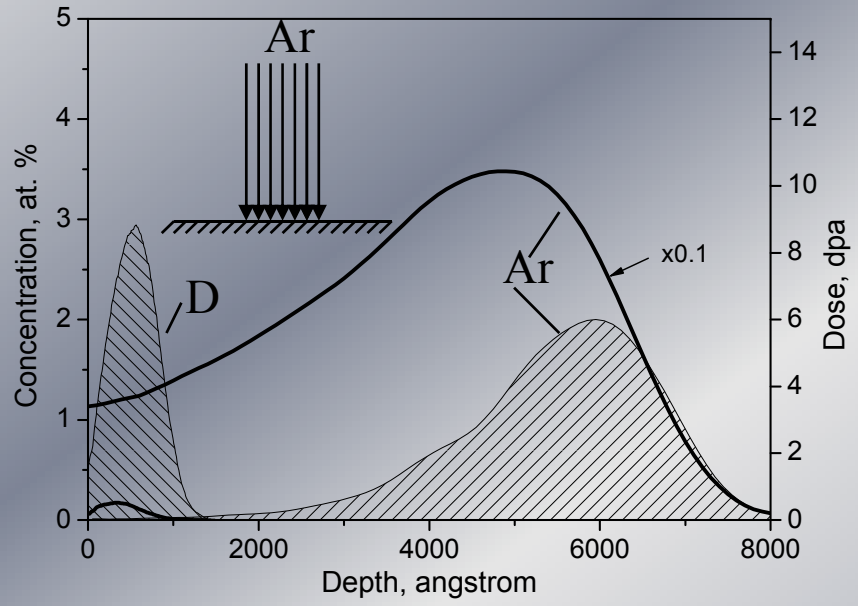

Only 40 dpa
at depth 0 -100nm

100 dpa + 0.5at.% Ar
at depth 0 – 100nm

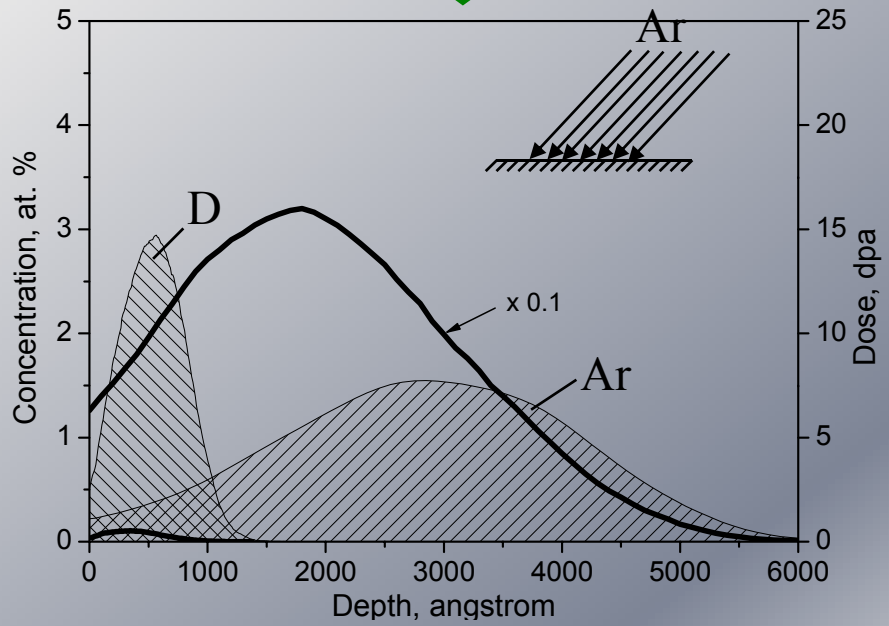

New task-Phase Stability of (Y, Al) Complex Example-Oxide Particles in 19Cr-2W-4Al ODSS

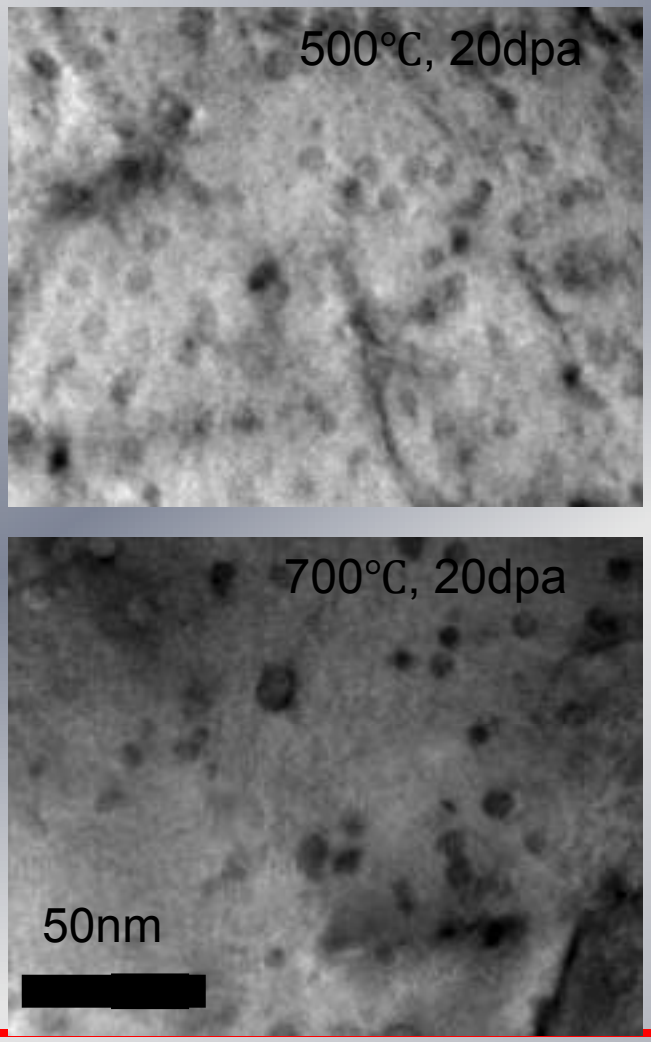

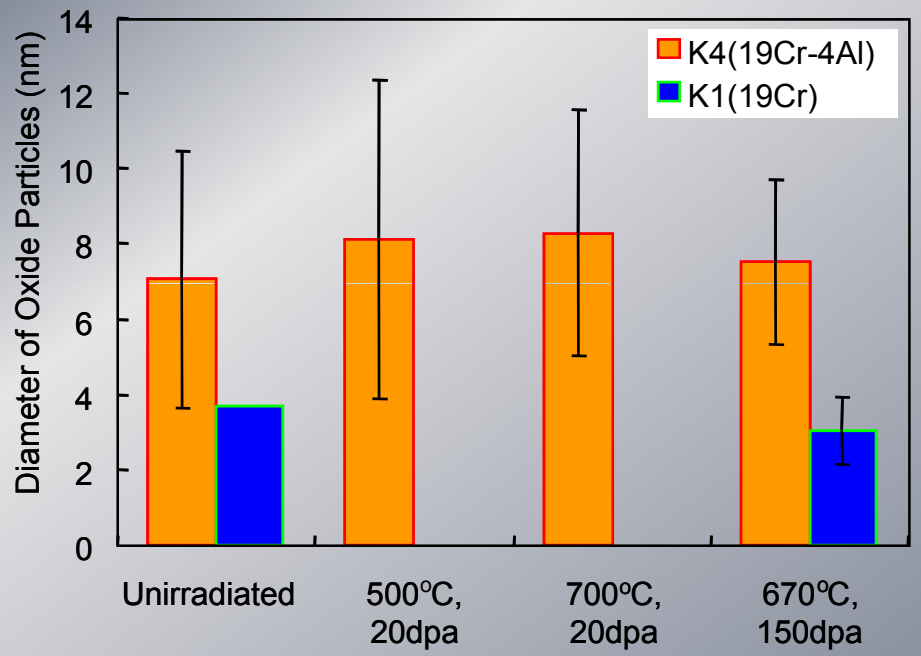

Averaged diameter of (Y, Al) complex oxides in 19Cr-2W-4Al ODS steel after ion-irradiation

No significant modification of oxide particles was observed after ion-irradiation up to 150dpa at 700 °C

(A. Kimura, 2007)

Fe-18Cr-10Ni-Ti

Single, dual and triple ion-beams : Cr^{3+}, He^{+} and H^{+} 50 dpa at 600ºC ESUVI facility

Accelerating Voltage Cr^{3+}, He^{+} and H^{+}: 1.8 MeV, 60 keV, 30 keV

- **1) single ion (Cr^{3+}): swelling 6%;**
- **2) dual ion (Cr^{3+} + He^{+}): swelling 6.5%;**
- **3) dual ion (Cr^{3+} + H^{+}) : swelling of 12%;**
- **4) triple ion (Cr^{3+} + He^{+} + H^{+}): experiments are doing now…**

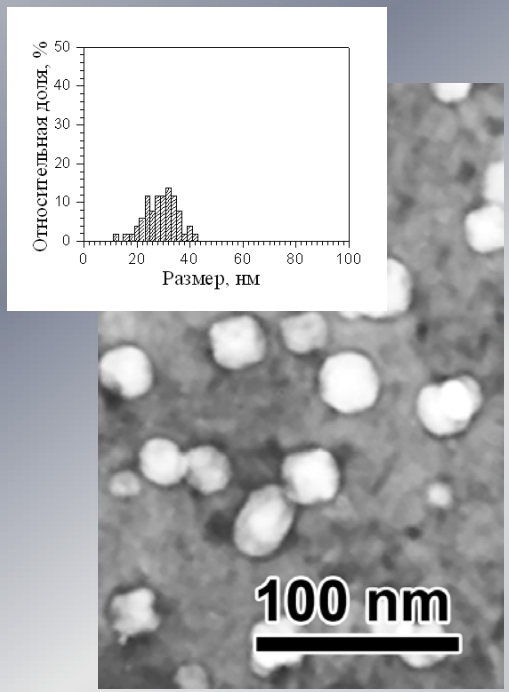

Cr

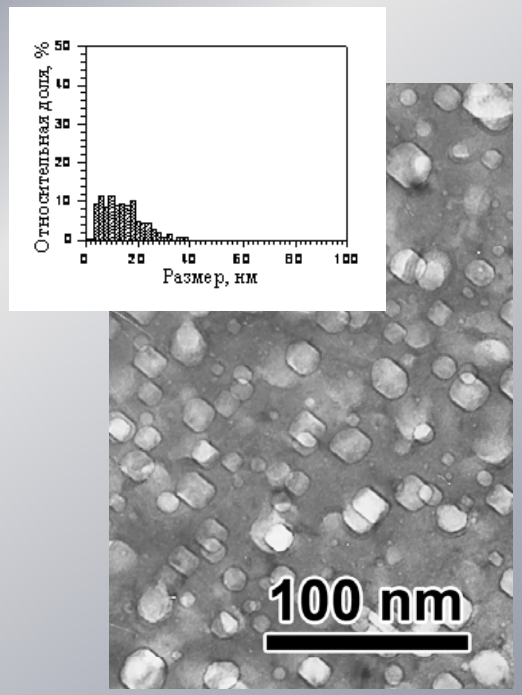

Cr + 60 кеВ He
1000 appm

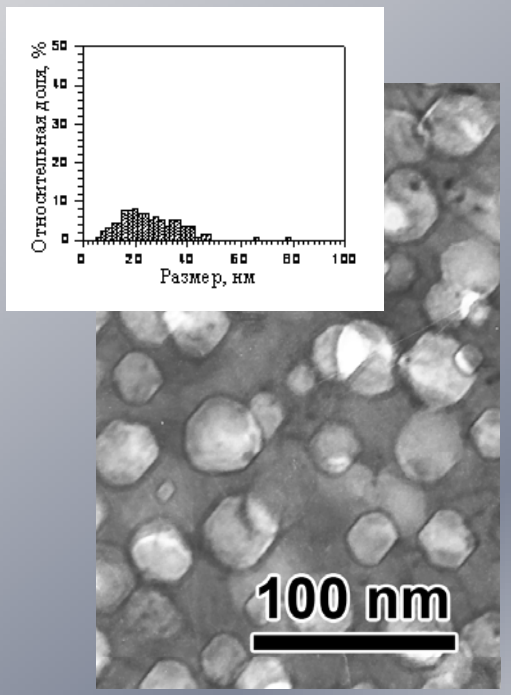

Cr + 30 кеВ H_2
2000 appm

Initial microstructure of EI – 852 steel

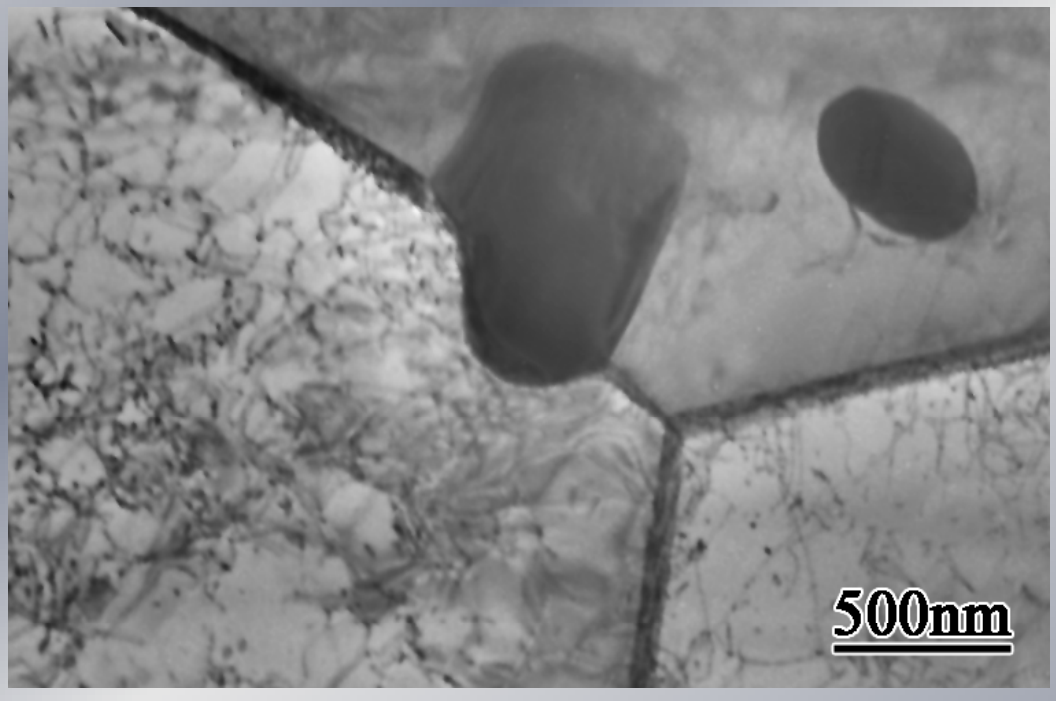

Irradiation	Void size , nm	Concentration, cm^{-3}	Swelling, %
Cr^{+5}	15-60	$4{,}0 \cdot 10^{13}$	0.01
Cr^{+5}+He	15-50	$3 \cdot 10^{15}$	0.4
Cr^{+5}+H			
Cr^{+5}+He+H	10-50	$2.2 \cdot 10^{16}$	0.4

Irradiation on ESUVI
EI-852 steel
(Cr^{+5}, E=1,7 MeV, T_{irr}=480^{0}C, D=100 dpa)

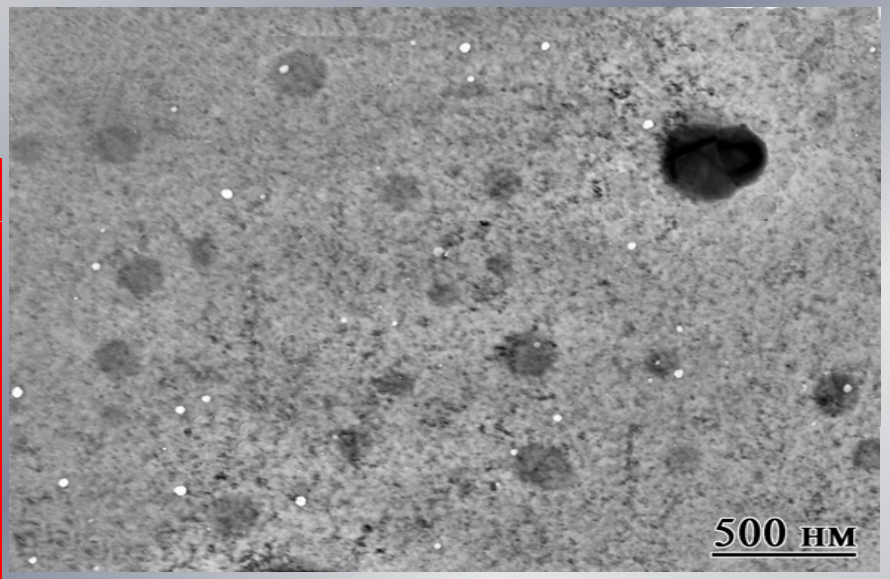

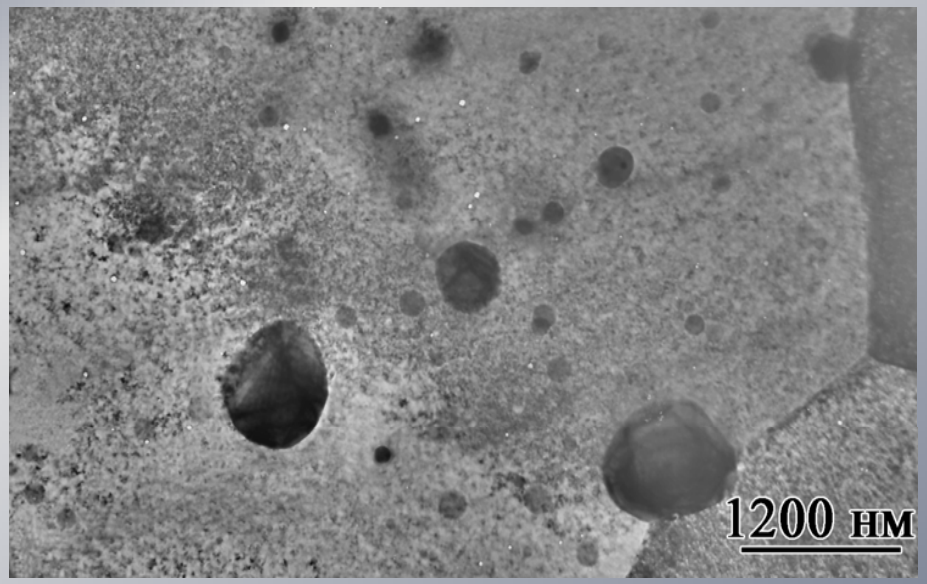

S=0.01%, p=4,0·10^{13}cm^{-3}, d=15-60 nm

Irradiation on ESUVI

EI-852 steel

(Cr^{+5}, E=1,7 MeV, T_{irr}=480^{0}C, D=100 dpa, He-3000appm)

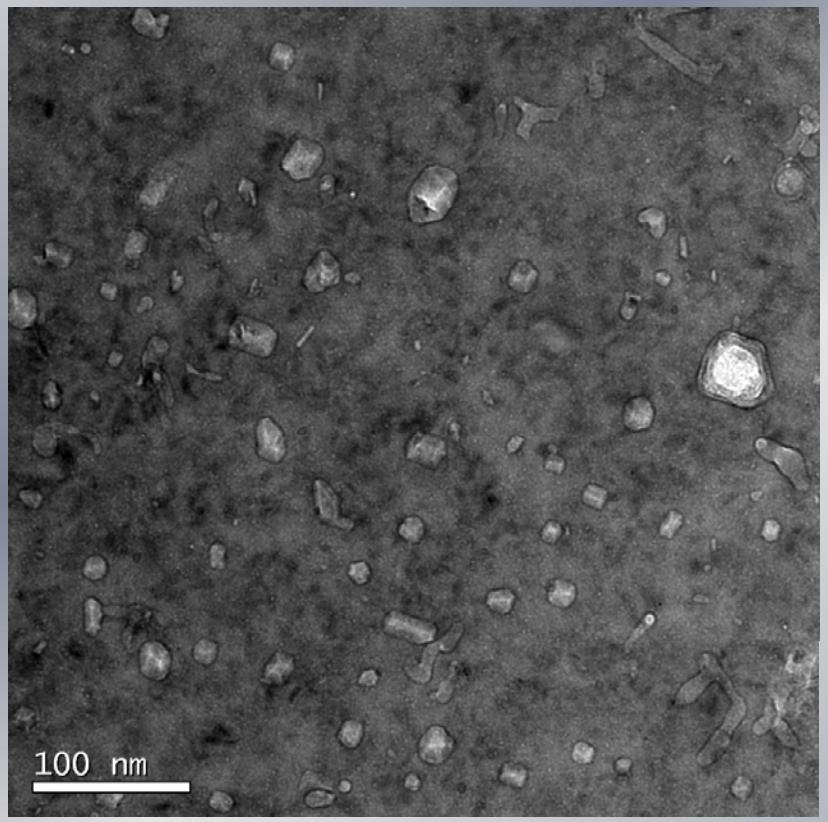

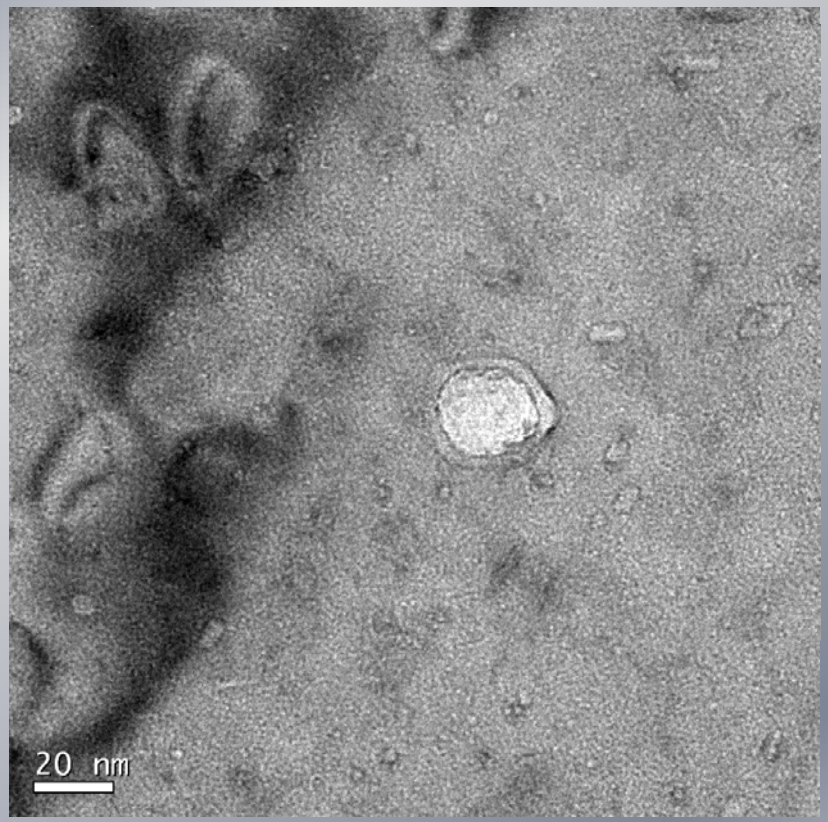

S=0.4%, p=3·10^{15}cm^{-3},d=15-50 nm

Irradiation on ESUVI
EI-852 steel
(Cr^{+5}, E=1,7 MeV, T_{irr}=480^{0}C, D=100 dpa, H-2000appm)

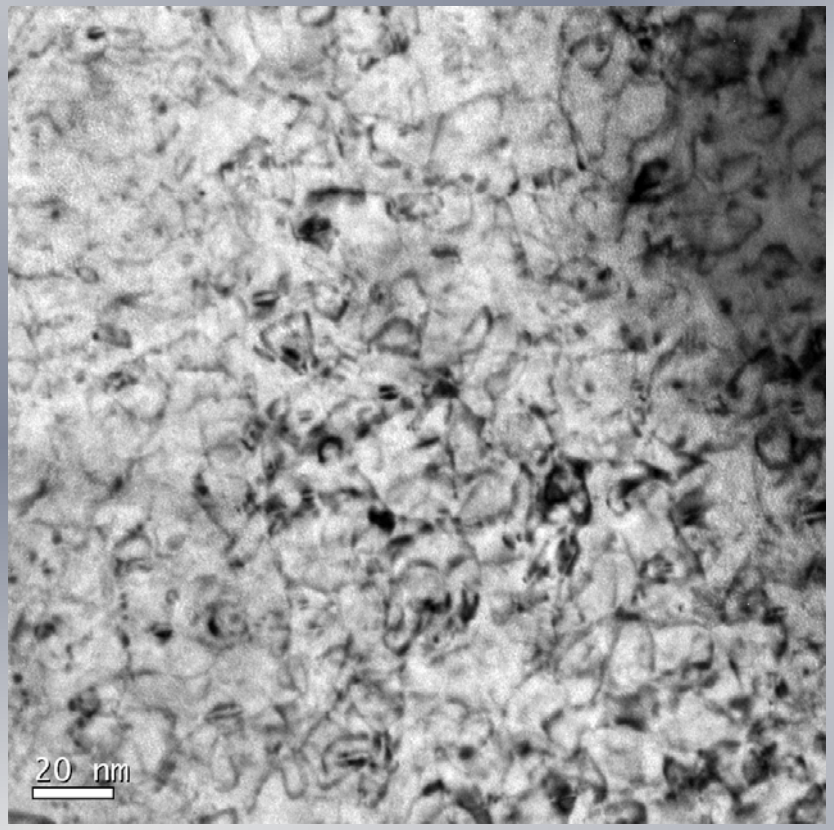

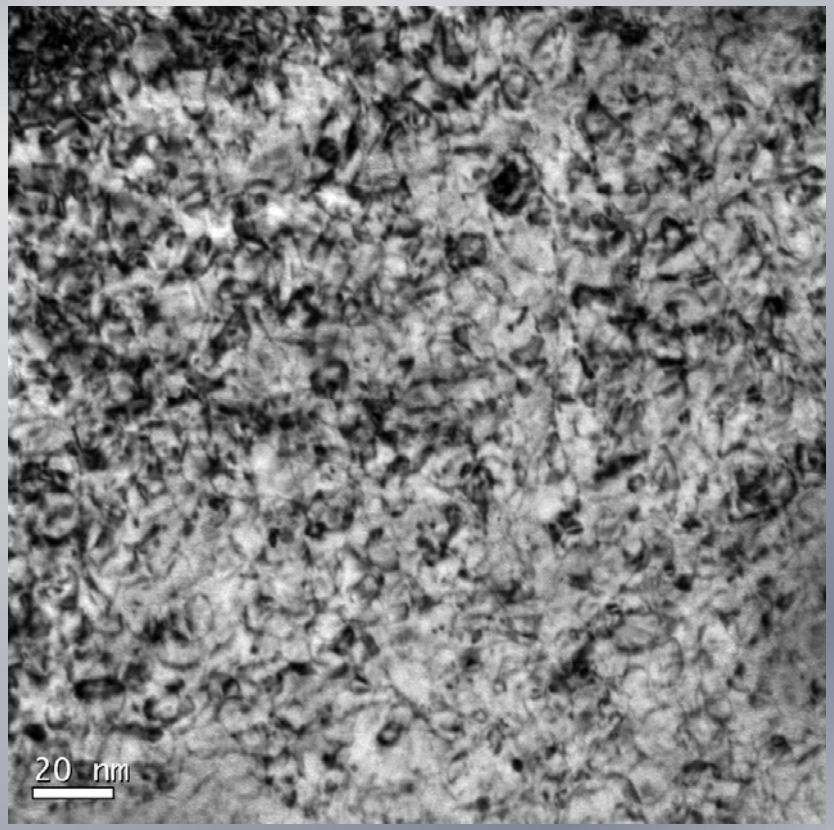

No cavities

Irradiation on ESUVI

EI-852 steel

(Cr^{+5}, E=1,7 MeV, T_{irr}=480^{0}C, D=100 dpa, He- 5000 appm H-8000appm)

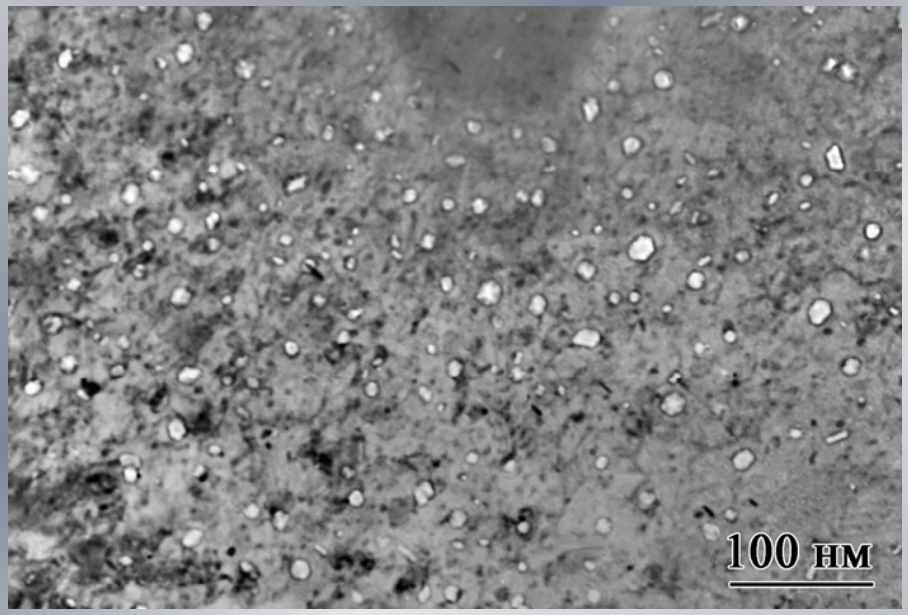

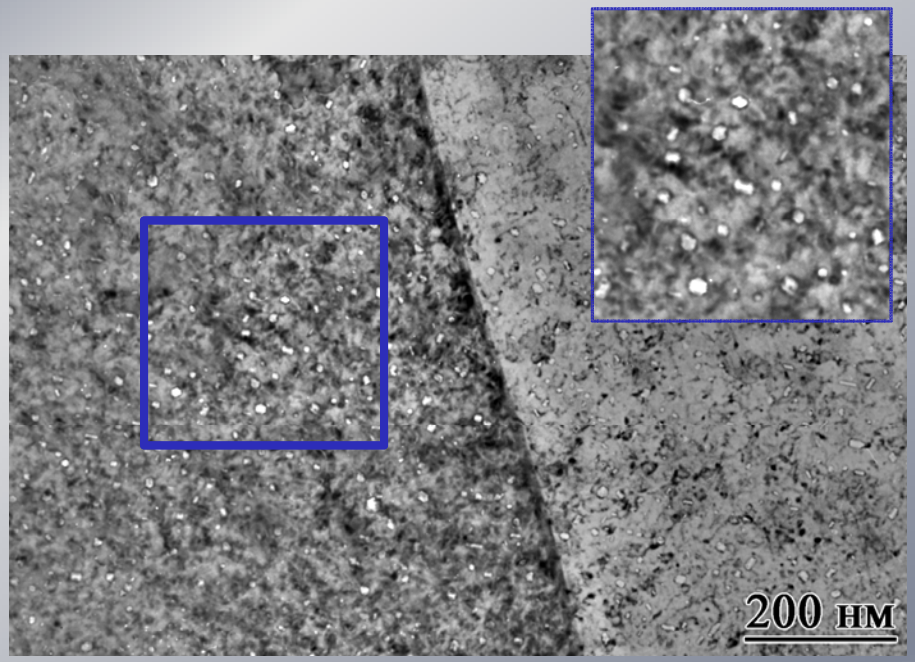

S=0.4%, p=2.2·10^{16}cm^{-3}, d=10-50 nm

Schematic drawing of triple beam irradiation system

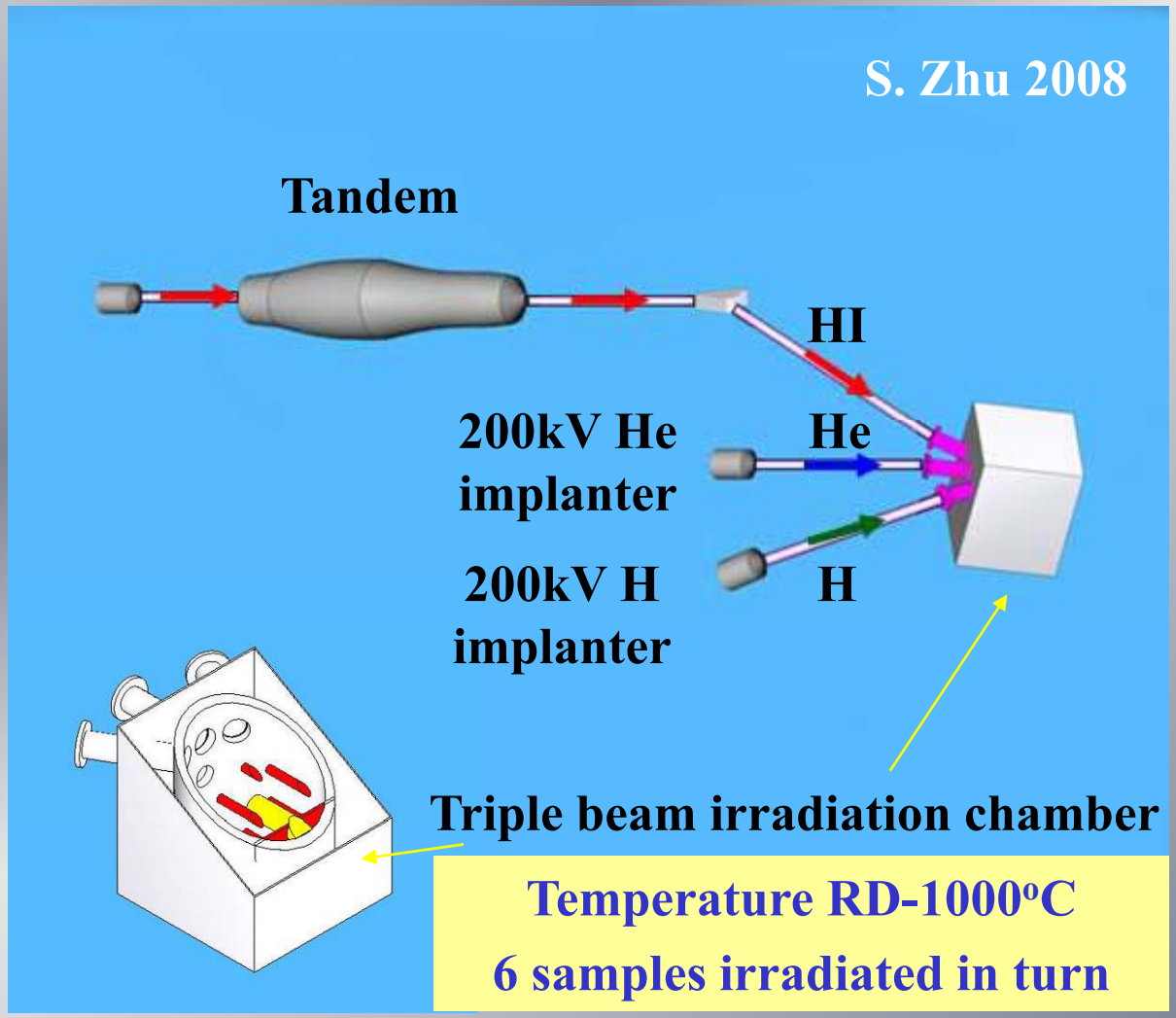

Design of the chamber and two implanters completed
Constructions are under way

JANNUS – CEA/Saclay site – general presentation (F. WILLAIME, 2008)

Main Goal: to simulate by ions the effects of neutron irradiation in materials

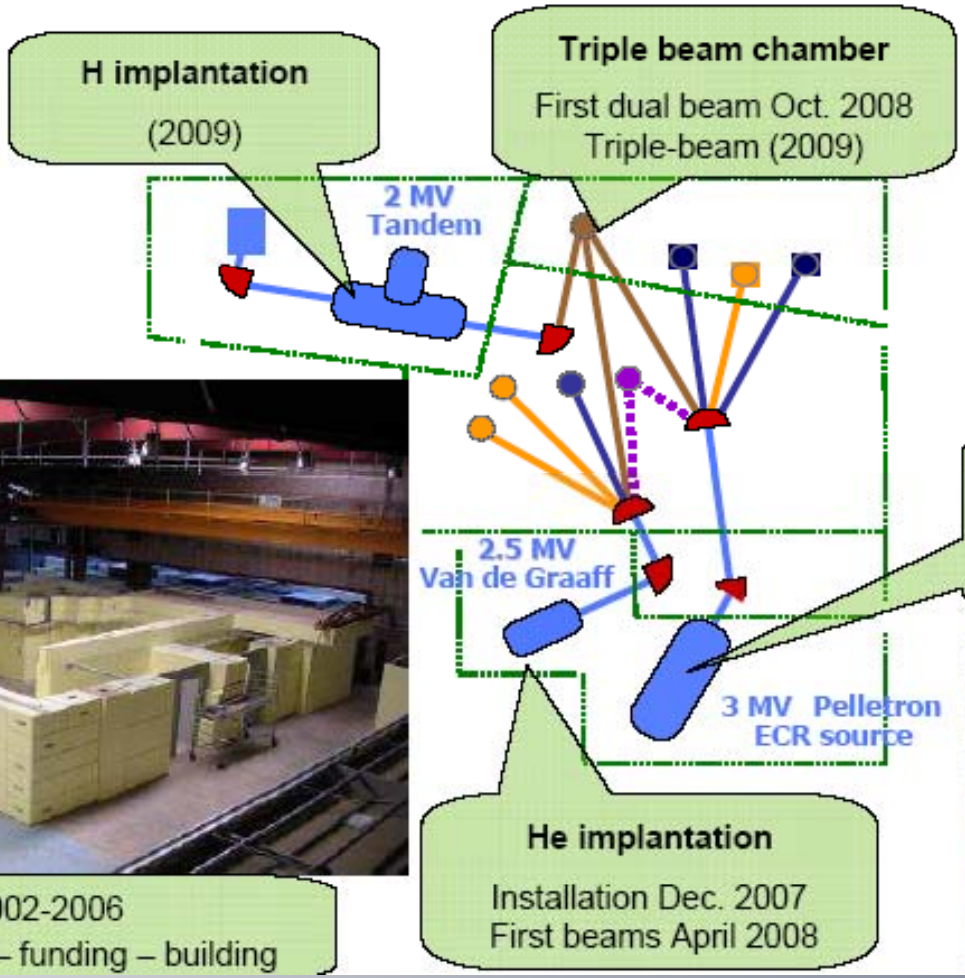

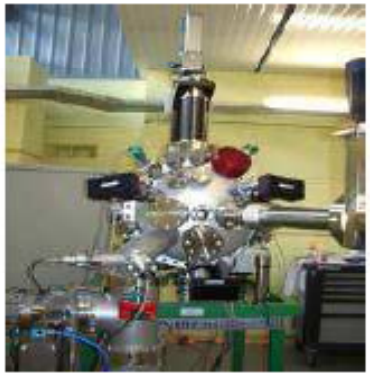

Proposed Experiments on model Fe/FeCr alloys

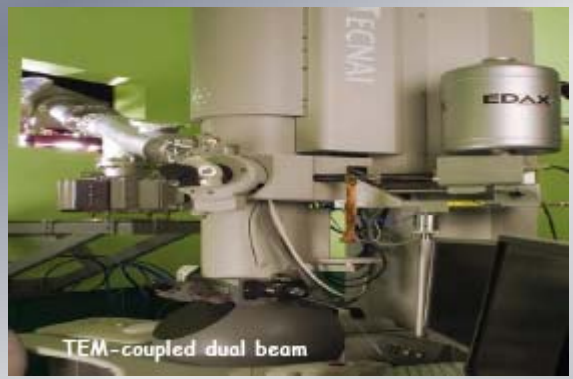

- **Irradiations (including « in-situ » in a TEM) in mono/dual and possibly triple beam mode using a wide range of experimental conditions :**
  - Temperature (largest range compatible with TEM characterization)
  - Total fluence, damage and/or implantation rates
- **Model Fe/FeCr alloys (EFDA materials): Fe, Fe C, Fe 5 10-14% Cr**
- **Quantitative microstructural characterization using TEM (number densities, sizes of bubbles/voids/dislocation loops) and possibly TAP (a/ a' unmixing, segregation) & EELS (segregation on bubble/cavities, measurements of He densities) …**
- **Tentative schedule:**
  - 2009 (second half): in-situ TEM and single beam irradiation/implantation experiments + TEM investigations
  - 2010: dual beam experiments (in/ex situ), TEM + possibly first TAP experiments
  - 2011: continuation of dual beam exp./microstructural investigations + possibly first triple beam irradiations

Features of two – stage irradiations

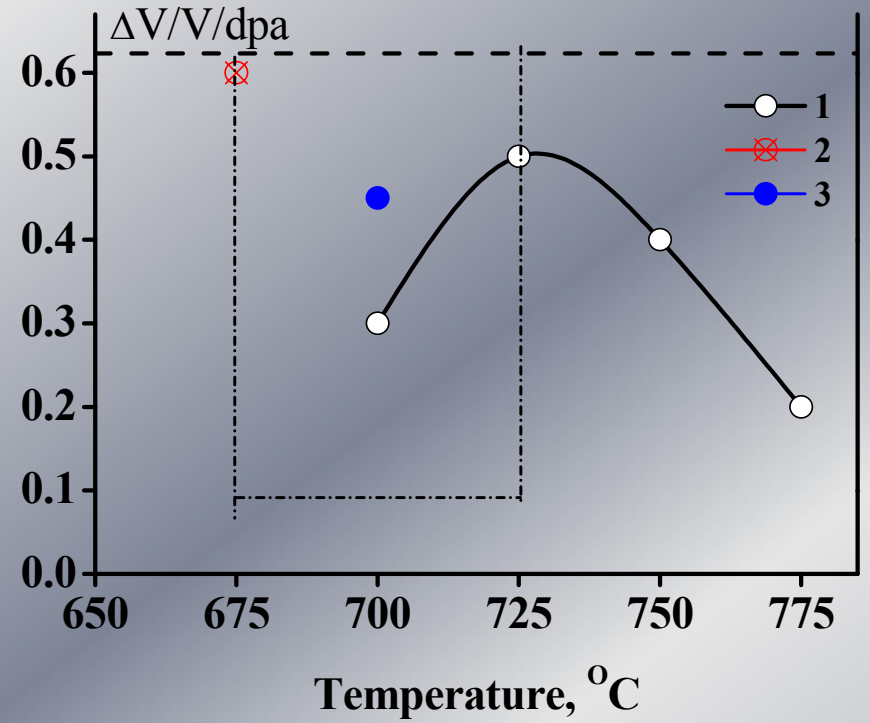

Temperature dependence of swelling rate of steel AISI316, deformed on 20% during two-stage irradiation(1). Irradiation rate during reactor irradiation at 585°C(2) and during ion irradiation at 625°C(3)

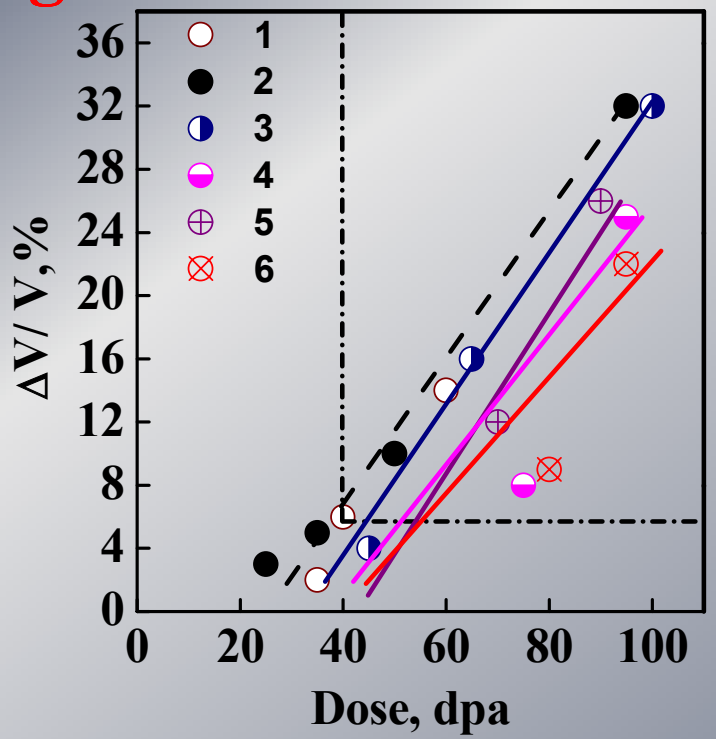

Swelling dependence of steel AISI316, deformed on 20% vs. dose during reactor irradiation at 585°C(1), ion irradiation at 625°C(2), and two-stage irradiation – reactor 43 dpa at 585°C and ior irradittion Ni^{2+} at 625°C(3), 650°C(4), 675 (5), 700°C

Dose dependence of swelling, concentration and size of voids in nickel during reactor and ion irradiation

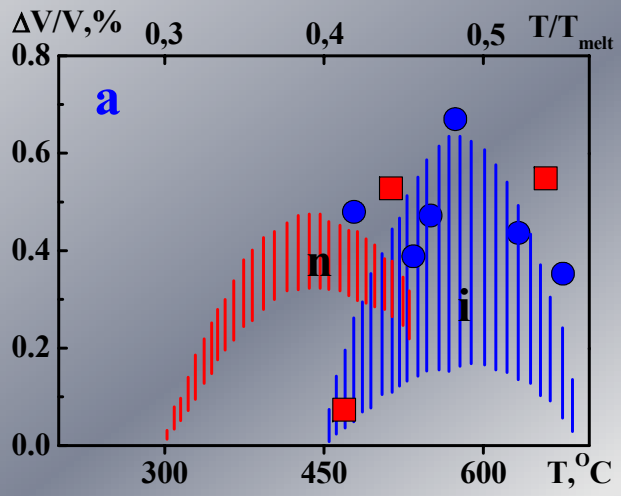

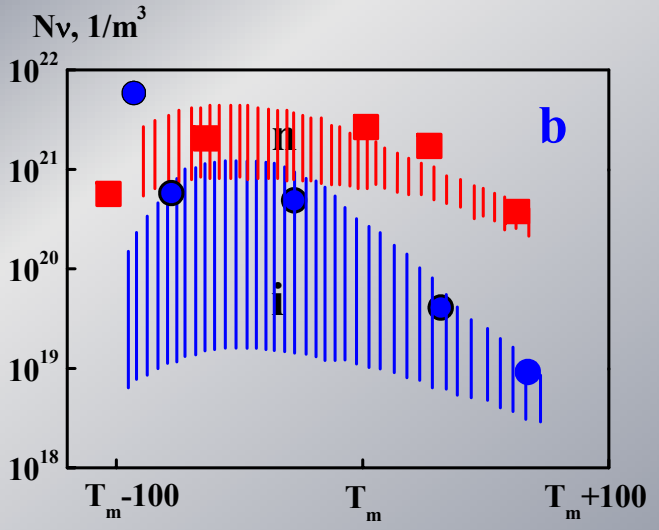

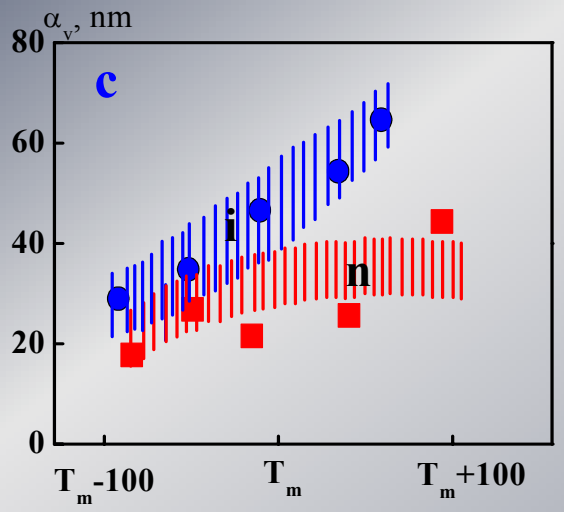

Dose dependence of swelling (a), concentration (b) and size of voids (c) in Nickel during reactor (n) and ion (i) (Ni^{2+} 4MeV) irradiation.

Ion irradiation with primary induced helium with quantity 20appm (■), with simultaneous induced helium (●): D= 1 dpa, C_{He}=20 appm

Temperature dependence of swelling of steel 16Cr15Ni3MoNb

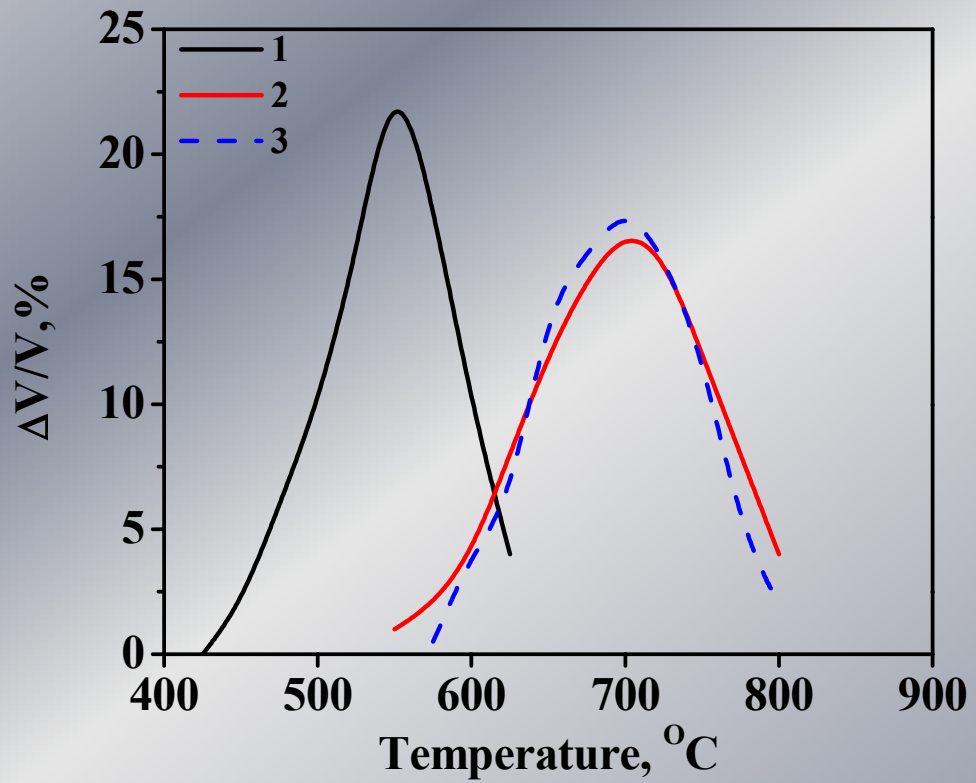

Temperature dependence of swelling 16Cr15Ni3MoNb steel :
1 – reactor irradiation ($\varphi t=2\cdot10^{27} n/m^2$);
2 – ion irradiation (Cr^{5+}, D=100 dpa);
3 – curve 1 displaced right on 140°C

Modeling of Irradiation behaviour of materials

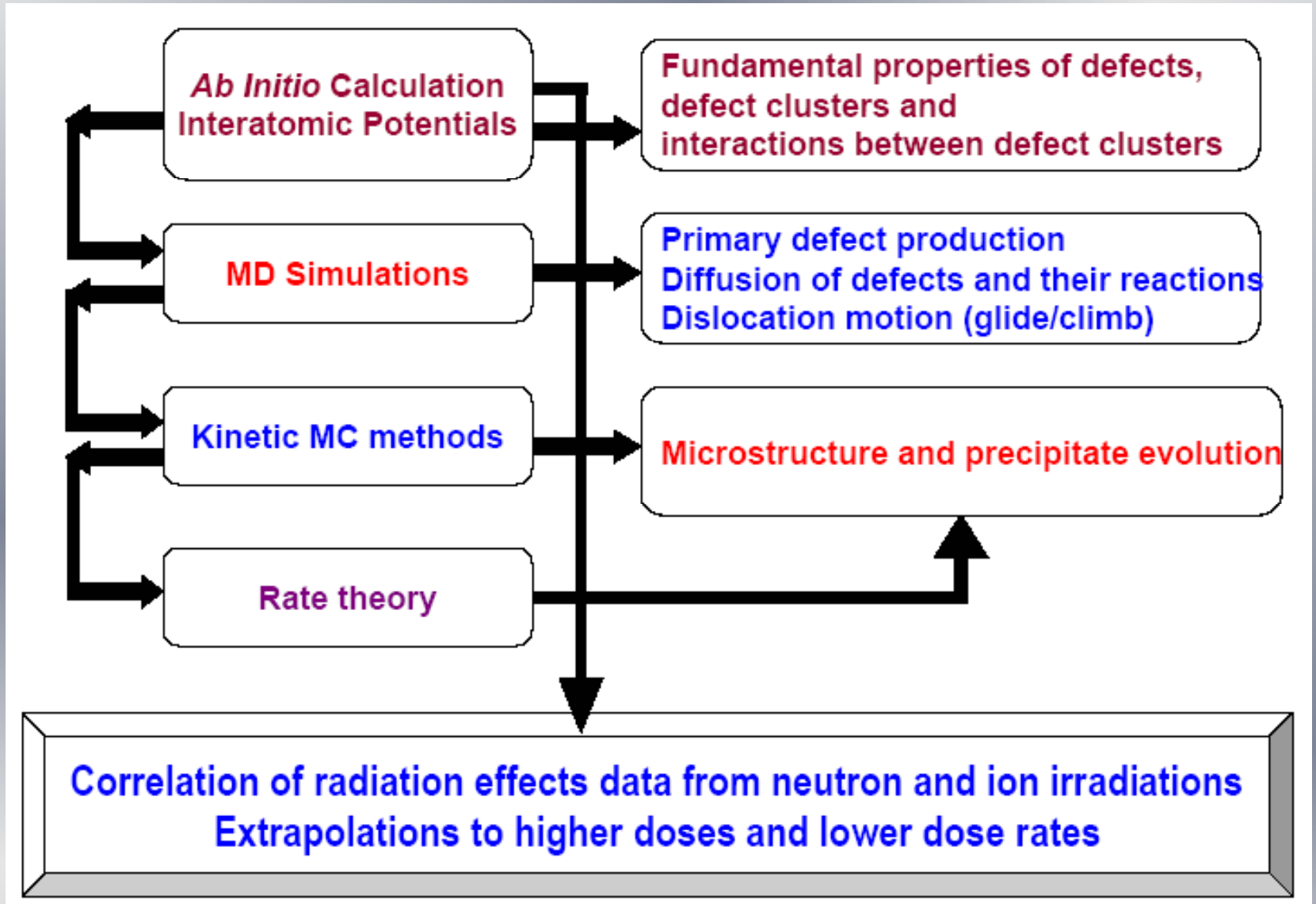

Summing ups of presentations and discussions

Need of some focal points

- New era for studies with ion-accelerators
  - with high-tech instrumentations
    - » FIB and nano indenters, microspecimen technologies needed for development of new materials and materials testing for fission and fusions, overcoming disadvantages of ion-accelerator based irradiation
    - » EXAFS, SANS, etc. for nano scale structural evolutions
    - » In-situ type experiments for dynamic understandings of radiation effects
- Empirical correlations between fission reactor irradiation / ion accelerator irradiation at very high doses (>120dpa)
  - Transcendental understanding of multi-scale modeling (proving effectiveness of ion-accelerator based irradiation studies)

CONCLUSIONS (continued)

- While neutron irradiations are essential to evaluate and qualify materials for Generation IV systems, it is important to note that effective radiation effects experiments can be performed using ion-beam facilities
- Charged particles irradiations can now provide a low-cost method for conducting valuable radiation effects research in absence of, or as a precursor to verification experiments in reactors.
- Main tasks of simulation experiments now are:
- Understanding of radiation damage mechanism of nuclear materials-better knowledge of the nature of point defects and interaction between them
- Set up the correlation between radiation-induced defects and material degradation mechanism
- Development of technology forestimating and predicting radiation damage
- Model predictions must be validated with advanced experimental techniques which are able to determine materials properties in a multiscale approach


Thank you for your attention!